:UNCLASSIFIED

Security Classification

AD 744660

DOCUMENT CONTROL DATA - R & D

(Security classification of title, body of abstract and indexing annotation must be entered when the overall report is classified)

1. ORIGINATING ACTIVITY (Corporate author) Numerical Analysis Research
Department of Mathematics
University of California
Los Angeles, Calif. 90024

2a. REPORT SECURITY CLASSIFICATION
UNCLASSIFIED

2b. GROUP

3. REPORT TITLE
NUMERICAL SOLUTION OF THE KROOK EQUATION FOR FLOW PAST A CYLINDER

4. DESCRIPTIVE NOTES (Type of report and inclusive dates)
Scientific Interim

5. AUTHOR(S) (First name, middle initial, last name)
Gerard Richter

6. REPORT DATE
July 1972

7a. TOTAL NO. OF PAGES
21 + 24 drawings

7b. NO. OF REFS
17

8a. CONTRACT OR GRANT NO.
N000-14-69-A-0200-4022

b. PROJECT NO.
044-144

c.

d.

9a. ORIGINATOR'S REPORT NUMBER(S)

9b. OTHER REPORT NO(S) (Any other numbers that may be assigned this report)

10. DISTRIBUTION STATEMENT
Approved for public release; distribution unlimited

11. SUPPLEMENTARY NOTES
To be submitted to the journal
The Physics of Fluids for publication

12. SPONSORING MILITARY ACTIVITY
Office of Naval Research - Code 432
Department of the Navy
Arlington, Virginia 22217

13. ABSTRACT

The Krook kinetic equation is used as the governing equation in an investigation of a class of exterior flow problems involving flow past an elliptic cylinder. A numerical method for solving the integral equation form of the Krook equation for this class of problems is described, and several sets of solutions are presented.

14. KEY WORDS

Elliptic cylinder problem
Flow past a circular cylinder
Flow past a finite flat plate

45

DD FORM 1 NOV 65 1473 (PAGE 1)
0102-014-6600

UNCLASSIFIED
Security Classification

Numerical Solution of the Krook Equation for Flow Past a Cylinder

Gerard Richter
Department of Mathematics
University of California, Los Angeles

ABSTRACT

The Krook kinetic equation is used as the governing equation in an investigation of a class of exterior flow problems involving flow past an elliptic cylinder. A numerical method for solving the integral equation form of the Krook equation for this class of problems is described, and several sets of solutions are presented.

I

LIST OF FIGURES

1. INTRODUCTION

The Krook kinetic equation [6] provides a useful characterization of many flow problems in kinetic theory. By integrating this equation along its characteristics, a coupled set of nonlinear integral equations for density, velocity and temperature can be obtained. This paper describes a numerical procedure which can be used to solve these integral equations for a class of exterior flow problems involving flow past an elliptic cylinder.

A simulation technique has been applied by Vogenitz et.al. to several exterior flow problems, including the leading edge problem [15] and flow past cylinders and spheres [14]. However, the only finite Knudsen number solutions of the kinetic equation to have been reported previously for exterior flow problems are those due to Huang et.al. [7-10], in which a discrete ordinate method was applied to the finite and semi-infinite flat plate problems.

The work reported here is part of a coordinated effort by several people to develop numerical procedures capable of yielding accurate solutions of the integral equations for a sequence of prototype problems in kinetic theory. Anderson [4,5] has solved the integral equations for several one-dimensional steady state problems, and Watanabe [16,17] has obtained numerical solutions for several time dependent problems. Apart from their intrinsic interest, these solutions can be used as standards in assessing the efficacy of approximate methods for solving the Boltzmann equation.

In §2, the integral equations are formulated in the context of the problem of a gas flowing past a circular cylinder. The free molecule

form of these equations is obtained in §3 and used in §4 in the development of a numerical method for solving the integral equations. Through the use of elliptic coordinates, this procedure is generalized in §5 to accomodate the case of an elliptic cylinder, one of whose axes is aligned with the free-stream direction. It is also shown that singularities develop at the front and rear stagnation points as the elliptic cylinder degenerates into a finite flat plate parallel to the freestream direction. In §6, free molecule solutions are presented for several freestream Mach numbers for elliptic cylinders ranging from a flat plate parallel to the freestream direction to a flat plate perpendicular to the freestream. In addition, finite Knudsen number solutions are presented for subsonic and mildly supersonic Mach numbers for elliptic cylinders deviating sufficiently from the flat plate limit.

2. FORMULATION OF THE INTEGRAL EQUATIONS

Consider the steady state flow of a rarefied gas past a stationary circular cylinder, as depicted in Figure 1.

For this problem, the Krook equation can be written in dimensionless form as follows:

$$\lambda\left(v_x \frac{\partial f}{\partial x} + v_y \frac{\partial f}{\partial y}\right) = \nu(\vec{x})\{F(\vec{v};\vec{x}) - f(\vec{v};\vec{x})\} . \qquad (1)$$

The parameter λ is the Knudsen number, $\nu(\vec{x})$ is a collision frequency depending on density and temperature, and $F(\vec{v};\vec{x})$ is a local Maxwellian distribution

$$F(\vec{v};\vec{x}) = \frac{n(\vec{x})}{(2\pi T(\vec{x}))^{3/2}} \exp -\left\{\frac{(\vec{v} - \vec{q}(\vec{x}))^2}{2T(\vec{x})}\right\} , \qquad (2)$$

where n, $\vec{q}$ and T are density, velocity and temperature, respectively. These, in turn, are given by the following moments of the distribution function:

$$n(\vec{x}) = \int d\vec{v}\, f(\vec{v};\vec{x})$$

$$\vec{q}(\vec{x}) = \frac{1}{n(\vec{x})} \int d\vec{v}\, \vec{v}\, f(\vec{v};\vec{x}) \qquad (3)$$

$$T(x) = \frac{1}{3n(\vec{x})} \int d\vec{v} |\vec{v} - \vec{q}(\vec{x})|^2 f(\vec{v};\vec{x}) \ .$$

In the foregoing formulation, the following nondimensionalization conventions have been implicitly assumed. The characteristic density and temperature are taken as their freestream values n_∞ and T_∞, and the characteristic length is taken as the cylinder radius R. Characteristic values of velocity and collision frequency are then defined by $\bar{u} = \sqrt{kT_\infty/m}$ and $\bar{\nu} = \nu(n_\infty, T_\infty)$, where k is Boltzmann's constant and m is the molecular mass. The Knudsen number is then given by $\lambda = R\bar{\nu}/\bar{u}$ and the freestream Mach number by $M_\infty = \sqrt{3/5}\, q_\infty$, where q_∞ is the dimensionless freestream velocity.

By an integration along its characteristics, the Krook equation can be formulated as a closed set of nonlinear integral equations for the low order moments - density, velocity and temperature. Using the notation of Anderson [3], these integral equations can be written

$$n(\vec{x}) = \frac{1}{\sqrt{2\pi}} \int_0^{2\pi} d\phi \left[n_B K_3\left(\frac{q_B}{\sqrt{T_B}}, \phi - \psi_B, \frac{c}{\lambda\sqrt{T_B}} \right) + \frac{1}{\lambda} \int_0^c dt\, \frac{n}{\sqrt{T}}\, K_2\left(\frac{q}{\sqrt{T}}, \phi - \psi, \frac{t}{\lambda\sqrt{T}} \right) \right]$$

$$n\vec{q} = \frac{1}{\sqrt{2\pi}} \int_0^{2\pi} d\phi \left[\hat{u}\, n_B \sqrt{T_B}\, K_4\left(\frac{q_B}{\sqrt{T_B}}, \phi - \psi_B, \frac{c}{\lambda \sqrt{T_B}} \right) \right.$$

$$\left. + \frac{1}{\lambda} \int_0^c dt\, n\, K_3\left(\frac{q}{\sqrt{T}}, \phi - \psi, \frac{t}{\lambda \sqrt{T}} \right) \right]$$

$$3nT + nq^2 = \frac{1}{\sqrt{2\pi}} \int_0^{2\pi} d\phi \left[n_B T_B \left\{ K_5\left(\frac{q_B}{\sqrt{T_B}}, \phi - \psi_B, \frac{c}{\lambda \sqrt{T_B}} \right) \right. \right. \qquad (4)$$

$$\left. \left. + K_3\left(\frac{q_B}{\sqrt{T_B}}, \phi - \psi_B, \frac{c}{\lambda \sqrt{T_B}} \right) \right\} \right.$$

$$\left. + \frac{1}{\lambda} \int_0^c dt\, n \sqrt{T} \left\{ K_1\left(\frac{q}{\sqrt{T}}, \phi - \psi, \frac{t}{\lambda \sqrt{T}} \right) + K_2\left(\frac{q}{\sqrt{T}}, \phi - \psi, \frac{t}{\lambda \sqrt{T}} \right) \right\} \right] .$$

These equations relate the flow properties at a point $\vec{x} = (r,\theta)$ to integrals over the flow field as viewed from $\vec{x}$. We thus have a radial (t) integration along characteristics passing through $\vec{x}$ and an angular (ϕ) integration over all such characteristics. For a given angle ϕ, we integrate radially along the characteristic

$$\vec{x}' = \vec{x} - s\hat{u} \qquad (5)$$

where $\hat{u}$ makes an angle ϕ with the x-axis. Along this characteristic, t is given by

$$t \equiv \int_0^s ds\, \nu(\vec{x} - s\hat{u}) , \qquad (6)$$

and c is the value of t at s = b, the distance traversed until a boundary is intercepted. Also, ψ is the angle between $\vec{q}$ and

and the x-axis, and the kernel functions are given by

$$K_n(\alpha,\beta,\gamma) = H_n(\alpha \cos\beta,\gamma) \exp - \left\{ \frac{(\alpha \sin\beta)^2}{2} \right\}$$

$$H_n(p,q) = \frac{1}{\sqrt{2\pi}} \int_0^\infty du\, u^{n-2} \exp - \left\{ \left[\frac{(u-p)^2}{2} + \frac{q}{u} \right] \right\} . \quad (7)$$

In the derivation of equations (4), a complete accomodation boundary condition is assumed. Thus, at the boundary point $\vec{x} - b\hat{u}$, the distribution function for the outgoing stream of molecules has the Maxwellian form

$$F(\vec{v};\vec{x} - b\hat{u}) = \frac{n_B}{(2\pi T_B)^{3/2}} \exp - \left\{ \frac{(\vec{v} - \vec{q}_B)^2}{2T_B} \right\} \quad (8)$$

where $\vec{q}_B$ and T_B are the velocity and temperature of the boundary at the point $\vec{x} - b\hat{u}$ and n_B, a pseudo-density variable, is determined through the condition that there be no net momentum normal to the boundary. In the context of the cylinder problem, the requirement that the radial component of velocity vanish at the cylinder leads to the following integral relation for n_B

$$n_B(\theta) = - \frac{1}{\lambda \sqrt{T_B}} \int_{\theta+\frac{\pi}{2}}^{\theta+\frac{3\pi}{2}} d\phi \cos(\phi - \theta) \int_0^\infty dt\, n\, K_3\left(\frac{q}{\sqrt{T}}, \phi - \psi, \frac{t}{\lambda\sqrt{T}} \right) , \quad (9)$$

the integral on the right being evaluated at the point on the surface to which θ corresponds.

The solid angle subtended by the cylinder at the point (r,θ) is described by the cone of influence angles

$$\phi_{1,2} = \theta \pm \text{Arcsin}\left(\frac{1}{r}\right) . \qquad (10)$$

For $\phi \in (\phi_1, \phi_2)$, the corresponding characteristics intercept the cylinder a distance

$$b = r\cos(\phi - \theta) - \sqrt{1 - [r \sin(\phi - \theta)]^2} \qquad (11)$$

away. For $\phi \notin (\phi_1, \phi_2)$, the corresponding characteristics do not intersect the cylinder and the radial integration extends over a semi-infinite range. In general, the angular integrand is discontinuous at ϕ_1 and ϕ_2.

Equations (4), in conjunction with (9), constitute a closed coupled set of nonlinear integral equations for n, $\vec{q}$, T and n_B. In addition, these integral equations are singular since $K_n(\alpha,\beta,\gamma)'$ contains a term which behaves like $\gamma^{n-1} \ell n\, \gamma$ as $\gamma \to 0$ [3].

The collision frequency ν is commonly chosen as a function of density and temperature to match some continuum transport coefficient of a particular gas; however, there is no unequivocal recipe for this function. Moreover, the use of any such variable collision frequency model necessitates the repeated numerical evaluation of the transformation (6), which is embedded in the radial integration. While this problem can be handled in a straightforward manner, a prohibitively large computation expense would be required for the class of problems considered here. On the other hand, the assumption of constant collision frequency reduces the computation to an economically tractable level. The emphasis of the present work is primarily on the development of numerical methods capable of yielding accurate solutions of the kinetic equation, rather than attempting to model specific physical situations.

Therefore, the assumption of constant collision frequency will be implicit in all that follows.

3. THE FREE MOLECULE LIMIT

The free molecule solution to the circular cylinder problem has previously been obtained by Trepaud & Brun [13] and compared with experimental data. For our purposes, the free molecule limit furnishes useful information relevant to the problem of solving the integral equations numerically. In the collisionless limit $\lambda = \infty$, the integral equations reduce to the following closed form expressions:

$$n = 1 - \frac{1}{\sqrt{2\pi}} \int_{\phi_1}^{\phi_2} d\phi \, K_3(q_\infty, \phi, 0) + \frac{1}{2\pi} \int_{\phi_1}^{\phi_2} d\phi \, n_B$$

$$n\vec{q} = q_\infty \hat{i} - \frac{1}{\sqrt{2\pi}} \int_{\phi_1}^{\phi_2} d\phi \, \hat{u} \, K_4(q_\infty, \phi, 0) + \frac{1}{2\sqrt{2\pi}} \int_{\phi_1}^{\phi_2} d\phi \, \hat{u} \, n_B \sqrt{T_B} \qquad (14)$$

$$3nT + nq^2 = 3 + q_\infty^2 - \frac{1}{\sqrt{2\pi}} \int_{\phi_1}^{\phi_2} d\phi [K_5(q_\infty, \phi, 0) + K_3(q_\infty, \phi, 0)]$$

$$+ \frac{3}{2\pi} \int_{\phi_1}^{\phi_2} d\phi \, n_B T_B$$

where

$$n_B(\theta) = \frac{1}{\sqrt{T_B}} \left\{ \exp - \left(\frac{q_\infty^2 \cos^2 \theta}{2} \right) - \sqrt{\pi} \left(\frac{q_\infty \cos \theta}{2} \right) \operatorname{erfc} \left(\frac{q_\infty \cos \theta}{\sqrt{2}} \right) \right\} . \qquad (15)$$

As explicitly recognized in the above equations, the free molecule solution depends inherently on the cone of influence angles $\phi_{1,2} = \theta \pm \text{Arcsin}(1/r)$. Thus as $r \to \infty$, we anticipate that the free molecule

solution decays to its freestream limit like $1/r$, and that as $r \to 1$, the gradients of the flow variables approach infinity like $1/\sqrt{r-1}$. These effects stem directly from the geometric configuration of the boundary. As such, they may be expected to occur for finite Knudsen numbers which are sufficiently large that the "boundary" terms (i.e. those involving n_B, $\vec{q}_B$, T_B) in equations (4) are of the same order of magnitude as the integrals over the interior of the flow field.

4. METHOD OF SOLVING THE INTEGRAL EQUATIONS

The integral equations can be discretized by replacing the solution by an approximate form involving finitely many free parameters, replacing the integrals by quadrature formulae, and requiring that the residual - the extent to which the approximate solution fails to satisfy the integral equations - be minimized in some sense. For computational purposes, a collocation condition was adopted, the residual being required to vanish at a finite set of grid points. The values of the flow variables n, $\vec{q}$, T at these points are then used to interpolate the flow field over the rest of the domain. The numerical solution of the integral equations can thus be considered in three stages: (1) interpolation of the flow field; (2) discretization of the integrals; and (3) solution of the discrete equations.

Since the flow pattern for $y < 0$ is the mirror image of that for $y > 0$, we need only interpolate over the upper half plane portion of the domain; $r > 1$, $0 \leq \theta \leq \pi$. As previously noted, for sufficiently large Knudsen numbers, the flow field may be expected to vary roughly as $\mathrm{Arcsin}(1/r)$ in the radial direction. Accordingly, the radial coordinate is mapped into a bounded interval by means of the

transformation

$$\eta = \text{Arcsin}\left(\frac{1}{r}\right) , \tag{16}$$

and, as an additional means of controlling the distribution of grid points, bilinear transformations are applied to θ and η. In the transformed domain - a bounded rectangle - the flow variables are interpolated over a uniformly spaced set of grid points. A 4-point local Lagrangian scheme is used in the radial direction, while cubic spline interpolation is used in the angular direction. Both interpolation schemes entail approximation by piecewise cubic polynomials; in the latter case, the approximation has two continuous derivatives [1].

The integrals in equations (9) and (11) are discretized by means of composite low order Gaussian quadrature formulae. Gauss-Legendre quadrature is applied in subintervals in which the integrand is analytic, while special logarithmic and square root Gaussian formulae are applied in subintervals in which these singularities occur. To account for the discontinuities in the angular integrand at the cone of influence angles ϕ_1 and ϕ_2, separate formulae are applied to (ϕ_1, ϕ_2) and its complement, each of these intervals being allotted a number of subintervals in proportion to its length. A sequence of arithmetically expanding subintervals is used for the radial (t) composite. For infinitely extensive characteristics, the composite is applied over a finite interval $0 \leq t \leq t_{max}$. For $t > t_{max}$, the integrand is approximated by its freestream form, which can be integrated directly using the relation

$$\frac{\partial}{\partial\gamma} K_n(\alpha,\beta,\gamma) = -K_{n-1}(\alpha,\beta,\gamma) \ . \qquad (17)$$

The discretization of the integral equations typically yields a non-sparse system of several hundred simultaneous nonlinear algebraic equations. These equations are solved iteratively by means of Anderson's Extrapolation Algorithm [2], which entails a linearization of the successive substitution iteration function about several of the most recent iterates. The flow variables are assigned new values as soon as they become available, as in a Gauss-Seidel iteration. As λ decreases, the integral equations become more difficult to solve numerically because the kernel functions decay more rapidly. Hence, the best strategy for obtaining solutions of the integral equations for various values of λ is to start with the free molecule solution and proceed in the direction of decreasing λ, using as initial iterate for a particular value of λ, the solution corresponding to the next larger value.

Another crucial problem is the evaluation of the kernel functions. Since $H_n(p,q)$ must be computed repeatedly during the course of solving the integral equations numerically, it is imperative that this process be as efficient as possible. Thus the computational algorithm is as follows. The domain $|p| \leq 2$, $q > 0$ is mapped into a bounded rectangle with a bilinear transformation in q, and a rectangular grid of uniformly spaced points is laid down over the transformed domain. For $n = 2,3,4$, H_n is approximated over this domain by the bicubic Hermite polynomial which interpolates H_n, its first partial derivatives, and its mixed partial derivative at each of the grid points. Values of H_n for $n > 4$ are computed via the recurrence formula

$$H_n = pH_{n-1} + (n - 3)H_{n-2} + qH_{n-3} .$$

This completes our discussion of the numerical procedure used to solve the integral equations for the circular cylinder problem. This procedure can be generalized in straightforward fashion to elliptic cylinders, as described in the next section.

5. GENERALIZATION TO ELLIPTIC CYLINDERS

We now consider a more general class of exterior flow problems involving flow past an elliptic cylinder described by

$$\frac{x^2}{A^2} + \frac{y^2}{B^2} = 1 . \tag{19}$$

To facilitate the study of this class of problems, we use an elliptic coordinate system, which arises from the complex transformation $z = c \cosh \rho$. Equating the real and imaginary parts of this transformation and making the appropriate identifications, we obtain the following families of confocal ellipses and hyperbolas

$$\begin{aligned} &\frac{x^2}{\rho^2 - (1 - A^2)} + \frac{y^2}{\rho^2 - (1 - B^2)} = 1 \\ &\frac{x^2}{\cos^2 \mu} - \frac{y^2}{\sin^2 \mu} = A^2 - B^2 . \end{aligned} \tag{20}$$

In terms of this orthogonal coordinate system, the domain exterior to the elliptic cylinder is described by

$$-\pi < \mu \leq \pi, \qquad \rho > 1 .$$

Equations (9) and (11) still apply to this class of problems, although the cone of influence angles are now given by

$$\phi_{1,2} = \tan^{-1}\left\{ \frac{xy \mp \sqrt{B^2x^2 + A^2y^2 - A^2B^2}}{x^2 - A^2} \right\}, \qquad (21)$$

and θ in (11) must be regarded as the angle between the horizontal and the unit outer normal to the surface.

It can be shown that the cone of the influence of the elliptic cylinder varies like $1/\rho$ as $\rho \to \infty$, and like $c_1 + c_2\sqrt{\rho - 1}$ as $\rho \to 1$. Thus it is appropriate to use the transformation

$$\eta = \text{Arcsin}\left(\frac{1}{\rho}\right) \qquad (22)$$

for the interpolation of the solution. The rest of the numerical procedure is as previously described, and the generalization to elliptic cylinder is thus achieved.

It is instructive to consider the behavior of the free molecule solution to the elliptic cylinder problem as the elliptic cylinder degenerates into a flat plate parallel to the freestream direction. As $B \to 0$, all the curvature of the elliptic cylinder becomes concentrated at the front and rear stagnation points, and the cone of influence - and hence the free molecule solution - varies most markedly in the vicinity of these two points. In the limit $B = 0$, the cone of influence of the cylinder (in this case a flat plate) is not well-defined at the leading and trailing edges. Similarly, the limiting values of the flow variables as either of these two points is approached depends upon the direction of approach.

Free molecule solutions for a diffusely reflecting flat plate have previously been obtained by Ortloff [11]. However, these solutions are tainted by an incorrect expression for the distribution function. The correct free molecule form of the distribution function is

$$F(\vec{v};\vec{x}) = \begin{cases} \dfrac{1}{(2\pi)^{3/2}} \exp - \left[\dfrac{(\vec{v} - q_\infty \hat{i})^2}{2} \right], & \vec{v} \notin \Omega \\ \dfrac{n_B}{(2\pi T_B)^{3/2}} \exp - \left[\dfrac{v^2}{2T_B} \right], & \vec{v} \in \Omega , \end{cases}$$

where Ω is the cone of influence of the flat plate at the point $\vec{x}$.

The qualitative behavior of the singularities which occur for infinite Knudsen number should also be manifest at finite Knudsen numbers, since within regions of width $w << \lambda$ about the leading and trailing edges, the flow is essentially free molecular. Also, as $B \to 0$ (and likewise as $A \to 0$), the flow field approaches its singular limiting form, and the foregoing numerical procedure for obtaining finite Knudsen number solutions of the integral equation fails for "too oblong" elliptic cylinders.

6. NUMERICAL RESULTS

The integral equations were solved numerically for the sets of parameters listed in Table I. Up to 100 grid points were used to interpolate the flow field. Roughly ten or fewer iterations were required to satisfy a quasi-convergence criterion of 10^{-3}, while the time taken per iteration on the IBM 360/65 ranged as high as five minutes.

Figures 2-5 and 6-9 depict the flow of a gas past a circular cylinder at $q_\infty = 1.5$, which corresponds to a slightly supersonic

freestream Mach number. The first set of contour maps refers to the free molecule limit $\lambda = \infty$, while the second refers to $\lambda = 1$. Figures 10-12 present a comparison of the $\lambda = \infty$ and $\lambda = 1$ solutions along the rays $\theta = 0, \pi/2$ and π. The similarity of the two solutions stems from the fact that at $\lambda = 1$, the boundary conditions still have a direct influence on the interior flow pattern. However, the disturbance induced by the cylinder is more diffuse in the lower Knudsen number case. Thus, the square root singularity at the cylindrical surface is less conspicuous at $\lambda = 1$, and the flow variables approach their freestream limits more slowly. Also, the density in the shielded region behind the cylinder is considerably higher at $\lambda = 1$.

Figures 13-16 depict the flow pattern of a gas past an elliptic cylinder whose semi-minor axis is one-fourth the length of its semi-major axis. Essentially all the structure of the flow field is concentrated in the vicinity of the front and rear stagnation points, where the variation in the cone of influence of the cylinder is greatest. As the elliptic cylinder degenerates into a finite flat plate, it becomes increasingly difficult to interpolate the solution accurately in these two regions.

Figures 17-20 illustrate the free molecule solution for the aligned flow past a finite flat plate. The singularities at the leading and trailing edges are manifested in the coalescense of the contour lines at these two points. The free molecule solutions obtained by Ortloff [11] do not exhibit these singularities because an incorrect form was assumed for the distribution function. Figures 21-24 illustrate the free molecule flow pattern for the other extreme case of a flat plate perpendicular to the freestream direction. Both sets of free molecule

solutions are for $q_\infty = 3$, which corresponds to a freestream Mach number slightly greater than 2.

CONCLUDING REMARKS

The numerical procedure used to solve the integral equations is most suitable for high Knudsen number ($\lambda \gtrsim 1$), low Mach number ($M_\infty \lesssim 1$) flows. In this regime, the geometrical configuration of the boundary is of primary importance, and the flow field varies essentially as the cone of influence of the cylinder.

At lower Knudsen numbers, the "width" of the kernel functions decreases, and the effect of the boundary conditions on the interior flow pattern is less direct. More precisely, the boundary integrals in (4) at a fixed point $\vec{x}$ decrease in magnitude as $\lambda \to 0$. Thus a numerical method tailored to the variation of the cone of influence angles is not necessarily appropriate for solving the integral equations for low Knudsen numbers.

At higher Mach numbers, the gradients in the flow variables become larger, posing additional numerical difficulties. Due to the shielding effect of the cylinder, density may vary by several orders of magnitude. For example, the free molecule density at the rear stagnation point is of order $1/q_\infty \exp -(q_\infty^2/2)$ as $q_\infty \to \infty$ (this result can be obtained from equations (14) and (15)). Also, at finite Knudsen numbers, the occurrence of shock waves presents an added complication. The question of how to handle these effects numerically remains unresolved.

Also unsettled is the question of how to adapt the integral equation approach to the flat plate problem. It would seem that the singularities at the leading and trailing edges should be taken account of numerically,

yet it is unclear how this should be accomplished. At any rate, one cannot assume a priori that the effect of these singularities is negligible.

ACKNOWLEDGMENTS

The work described here constituted part of the author's Ph.D. thesis at Harvard University. Support was provided by National Science Foundation Grants GP-17383, GP-8666, GK-65 and by the Office of Naval Research under Contract N000-14-69-A-0200-4022. Reproduction in whole or in part is permitted for any purpose of the United States Government.

References

1. J. H. Ahlberg, E. N. Nilson, and J. L. Walsh, The Theory of Splines and Their Applications, Academic Press, New York, 1967.
2. D. G. M. Anderson, "On an Extrapolation Algorithm," Tech. Report. No. 18, Division of Engineering and Applied Physics, Engineering Sciences Laboratory, Harvard University, Cambridge, Mass. (1965).
3. D. G. M. Anderson, J. Fluid Mech. 26, 17-35 (1966).
4. D. G. M. Anderson, J. Plasma Physics 1, 255-265 (1967).
5. D. G. M. Anderson, J. Fluid Mech. 25, 271-287 (1966).
6. P. L. Bhatnagar, E. P. Gross, and M. Krook, Phys. Rev. 94, 511-524 (1954).
7. A. B. Huang and P. F. Hwang, Phys. Fluids 13, 309-317 (1970).
8. A. B. Huang, "Kinetic Theory of the Rarefied Supersonic Flow over a Finite Plate," in Rarefied Gas Dynamics, L. Trilling and H. Wachman, ed., Vol. 1, 529-544, Academic Press Inc., New York, 1969.
9. A. B. Huang and P. F. Hwang, "Kinetic Theory of the Sharp Leading Edge Problem, II, "Hypersonic Flow," paper RE 63, Oct. 1968, International Astronautic Federation, New York.
10. A. B. Huang and D. L. Hartley, Phys. Fluids 12, 96-108 (1969).
11. C. R. Ortloff, Phys. Fluids 10, 460-462 (1967).
12. G. R. Richter, Numerical Methods for Multi-dimensional Kinetic Theory Problems, Ph.D. Thesis, Harvard University, Cambridge, Mass. 1971.

13. P. Trepand and E. A. Brun, "A Study of Wakes Behind Cylinders in Free-Molecule Flow," in Rarefied Gas Dynamics, C. L. Brundin, ed., Vol. 2, 1177-1192, Academic Press Inc., New York, 1967.

14. F. W. Vogenitz, G. A. Bird, J. E. Broadwell, and H. Rungaldire, AIAA Journal 6, 2388-2394 (1968).

15. F. W. Vogenitz, J. E. Broadwell, and G. A. Bird, AIAA Journal 8, 504-510 (1970).

16. D. S. Watanabe, "Initial Value Problems for the Krock Equation, I, The Rayleigh Problem," Tech. Report No. 36, Division of Engineering and Applied Physics, Engineering Sciences Laboratory, Harvard University, Cambridge, Mass. (1971).

17. D. S. Watanabe, "Initial Value Problems for the Krook Equation, II, The Piston Problem," Tech. Report No. 37, Division of Engineering and Applied Physics, Engineering Sciences Laboratory, Harvard University, Cambridge, Mass. (1971).

TABLE I

λ	q_∞	T_B	A	B
∞	1	1	1	1
10	1	1	1	1
1	1	1	1	1
∞	1.5	1	1	1
10	1.5	1	1	1
1	1.5	1	1	1
∞	1	1	1	.25
10	1	1	1	.25
1	1	1	1	.25
∞	1	1	.5	1
10	1	1	.5	1
1	1	1	.5	1
∞	3	1	1	0
∞	3	1	0	1

Parameter values for elliptic cylinder problem

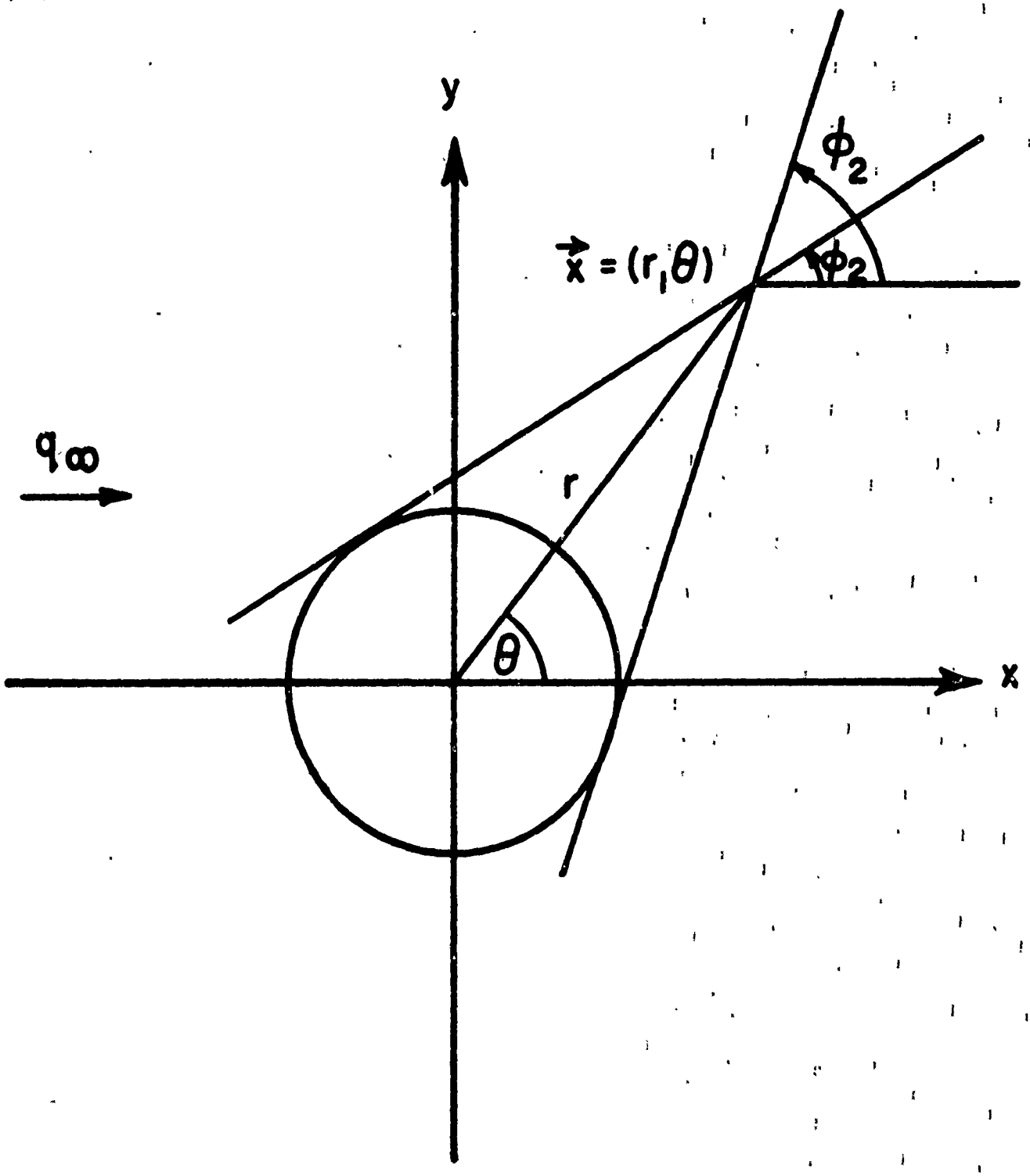

FIG. 1 FLOW PAST A CIRCULAR CYLINDER

FLOW PAST A CIRCULAR CYLINDER

$\lambda = \infty$ $Q_\infty = 1.5$ $T_B = 1$

DENSITY CONTOURS

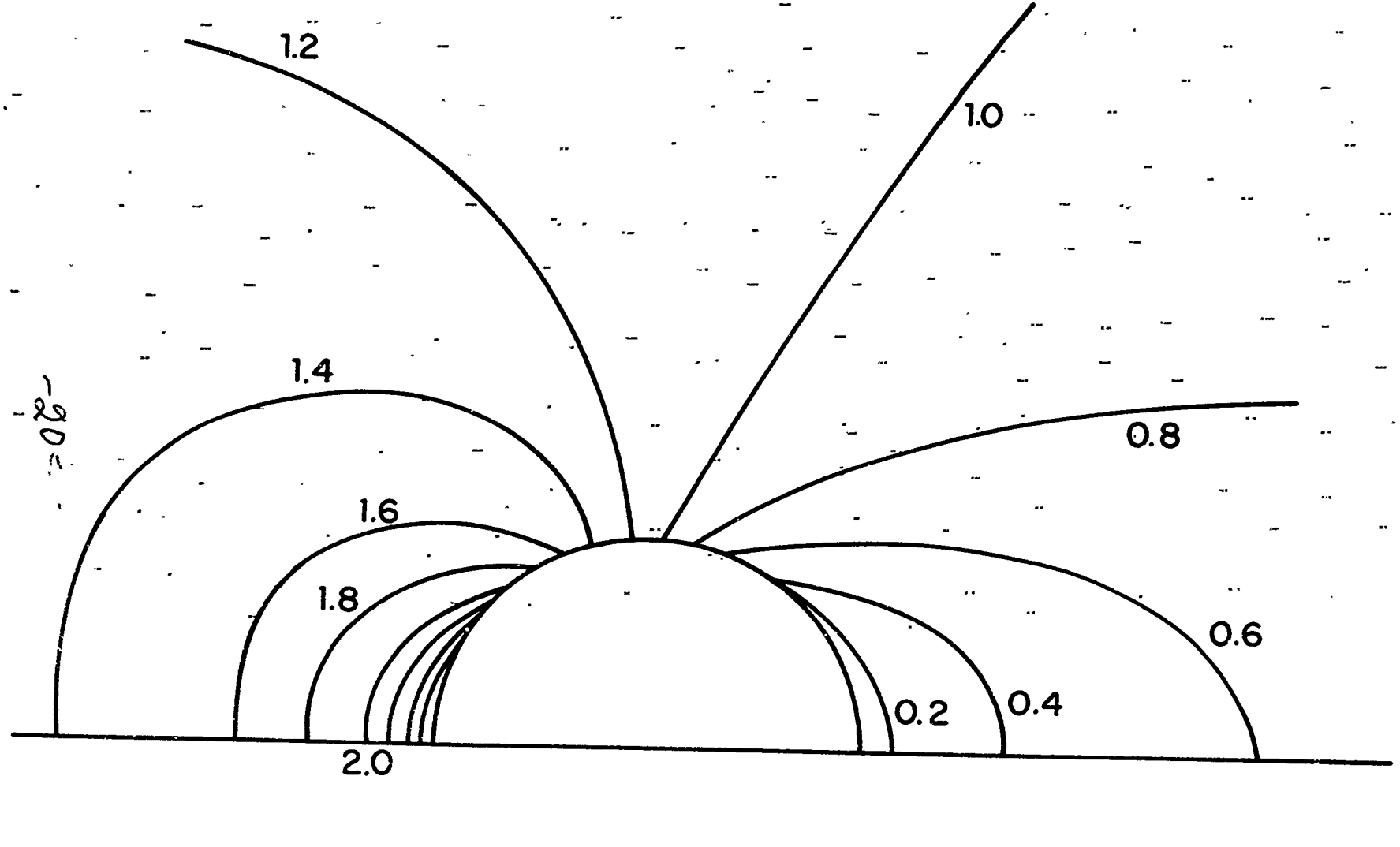

FIG. 2

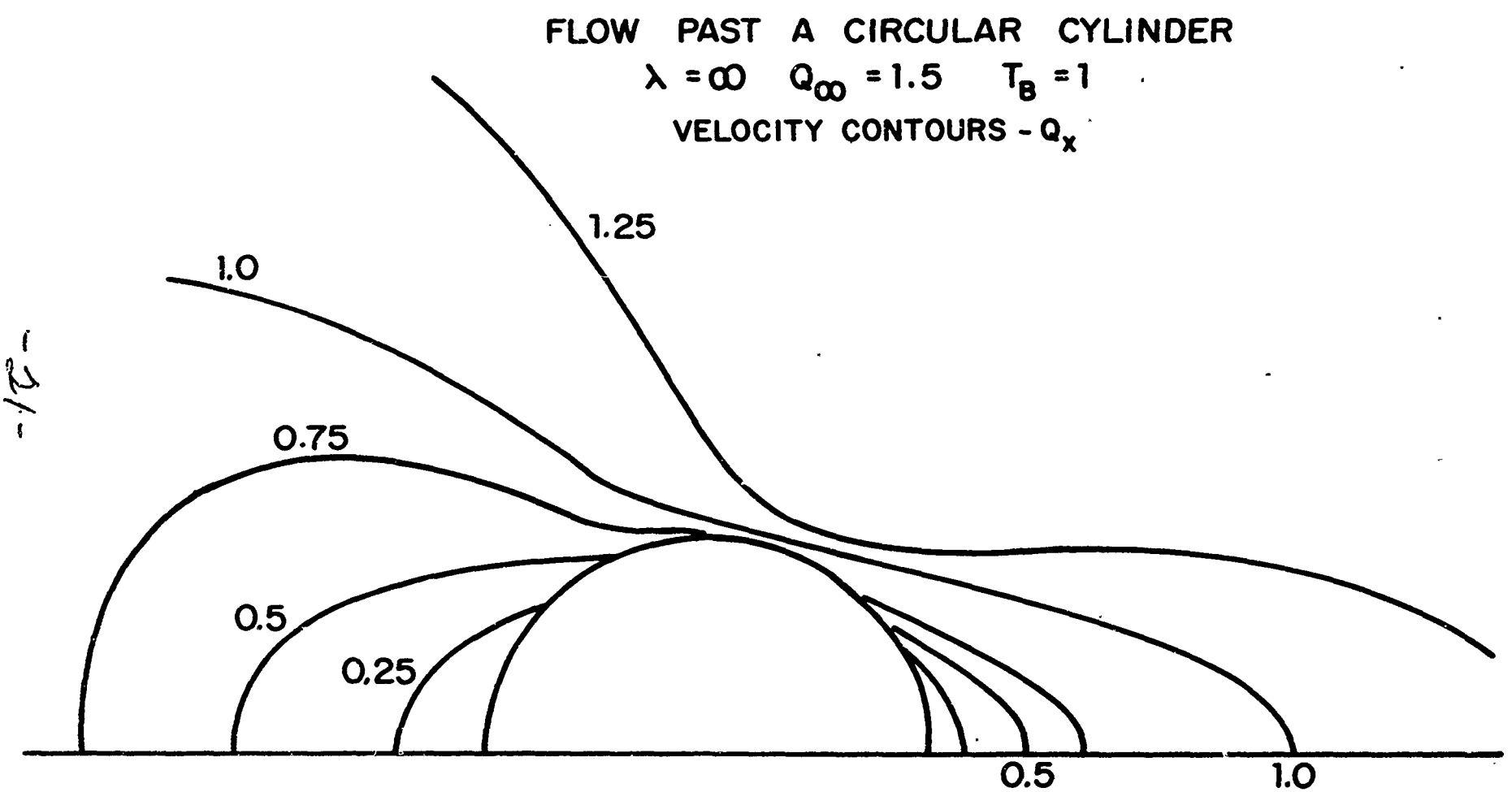
FLOW PAST A CIRCULAR CYLINDER
λ = ∞ Q∞ = 1.5 TB = 1
VELOCITY CONTOURS - Qx
1.25
1.0
0.75
0.5
0.25
0.5
1.0

FIG. 3

FLOW PAST A CIRCULAR CYLINDER

$\lambda = \infty \quad Q_\infty = 1.5 \quad T_B = 1$

VELOCITY CONTOURS - Q_y

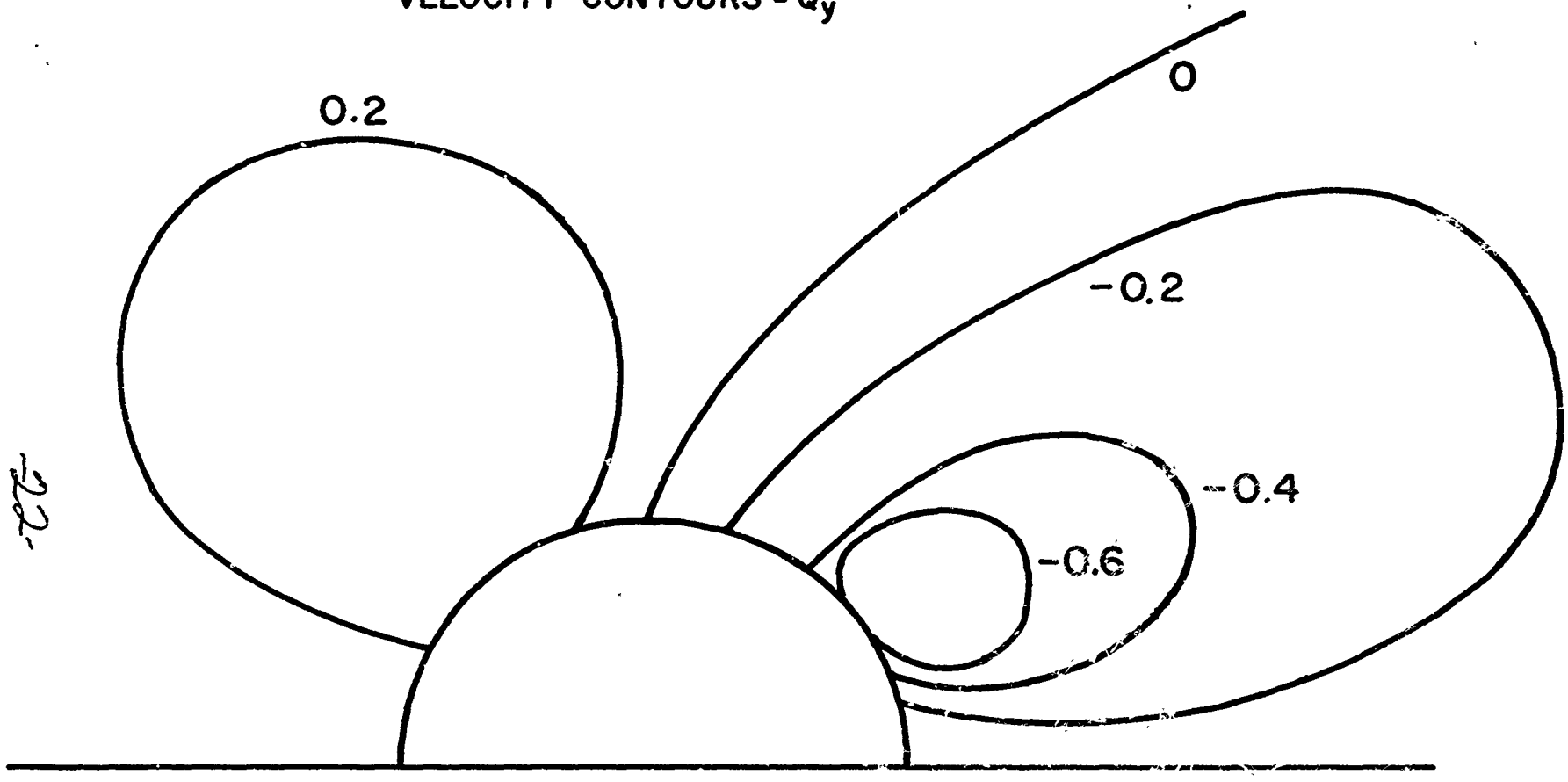

FIG. 4

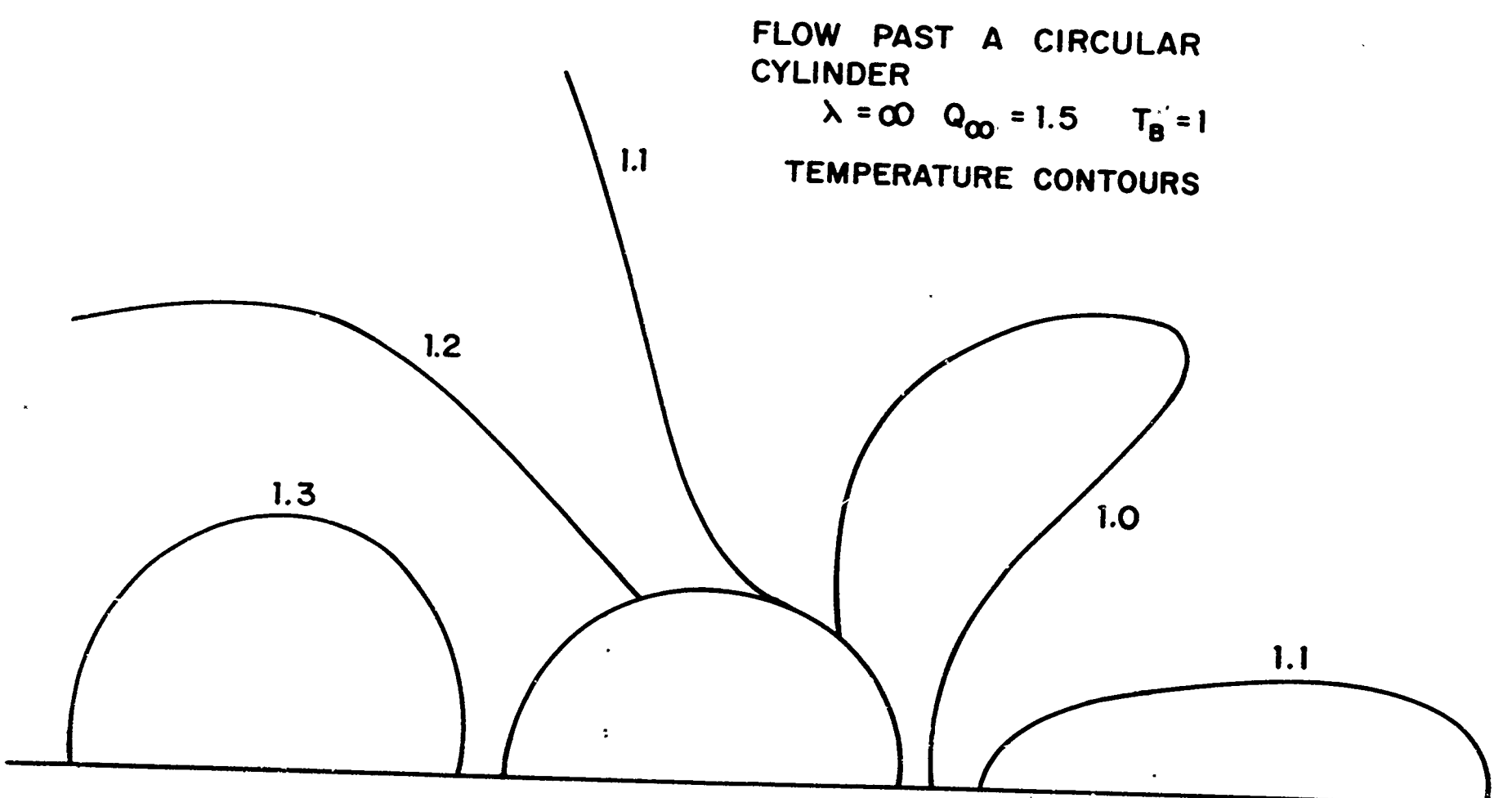
FLOW PAST A CIRCULAR CYLINDER
$\lambda = \infty$ $Q_\infty = 1.5$ $T_B = 1$
TEMPERATURE CONTOURS
1.1
1.2
1.3
1.0
1.1

FIG. 5

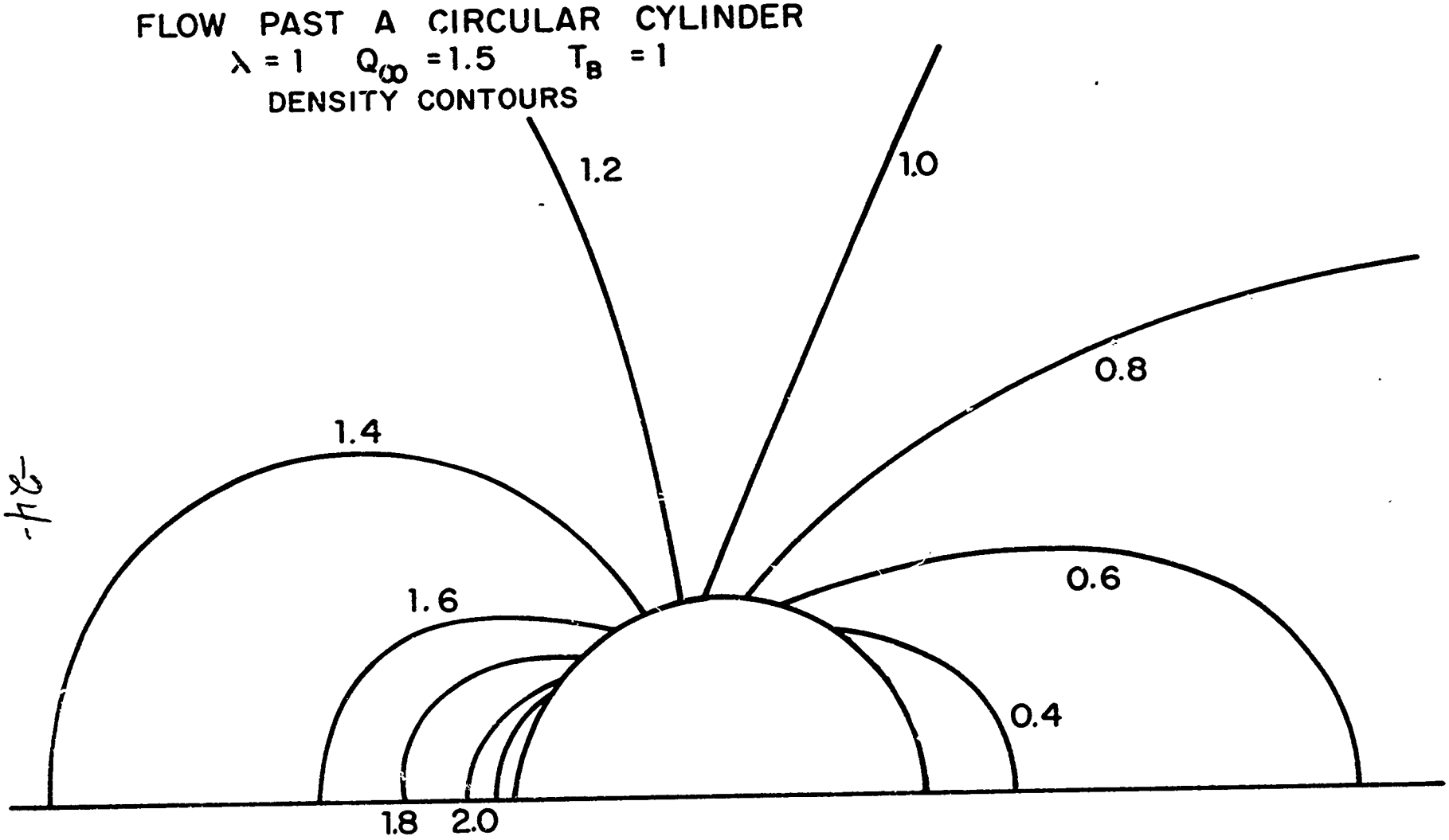
FLOW PAST A CIRCULAR CYLINDER
λ = 1 Q_∞ = 1.5 T_B = 1
DENSITY CONTOURS
1.2
1.0
0.8
1.4
0.6
1.6
0.4
1.8
2.0

FIG. 6

FLOW PAST A CIRCULAR CYLINDER

$\lambda = 1 \quad Q_\infty = 1.5 \quad T_B = 1$

VELOCITY CONTOURS - Q_x

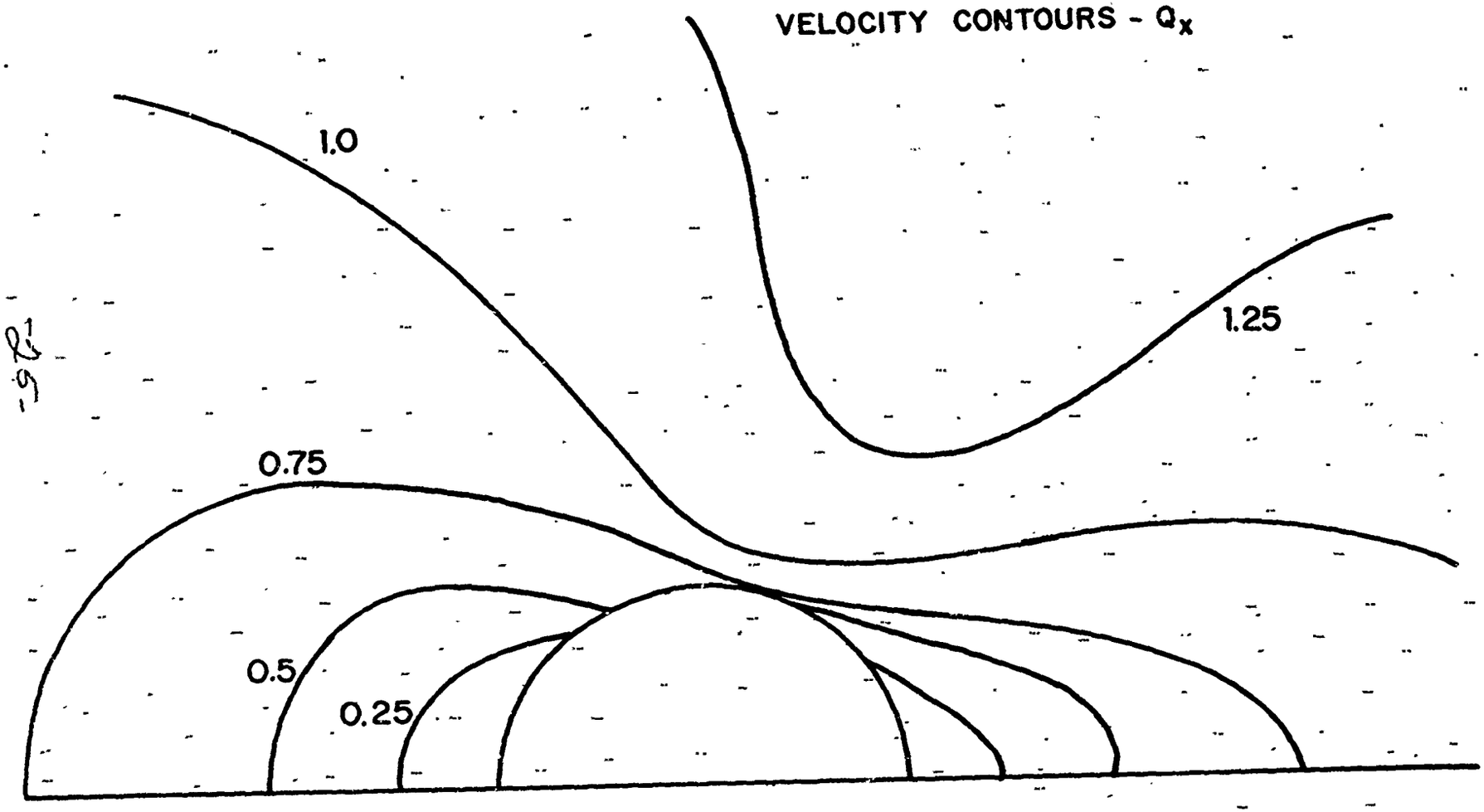

FIG. 7.

FLOW PAST A CIRCULAR CYLINDER

$\lambda = 1 \quad Q_\infty = 1.5 \quad T_B = 1$

VELOCITY CONTOURS - Q_y

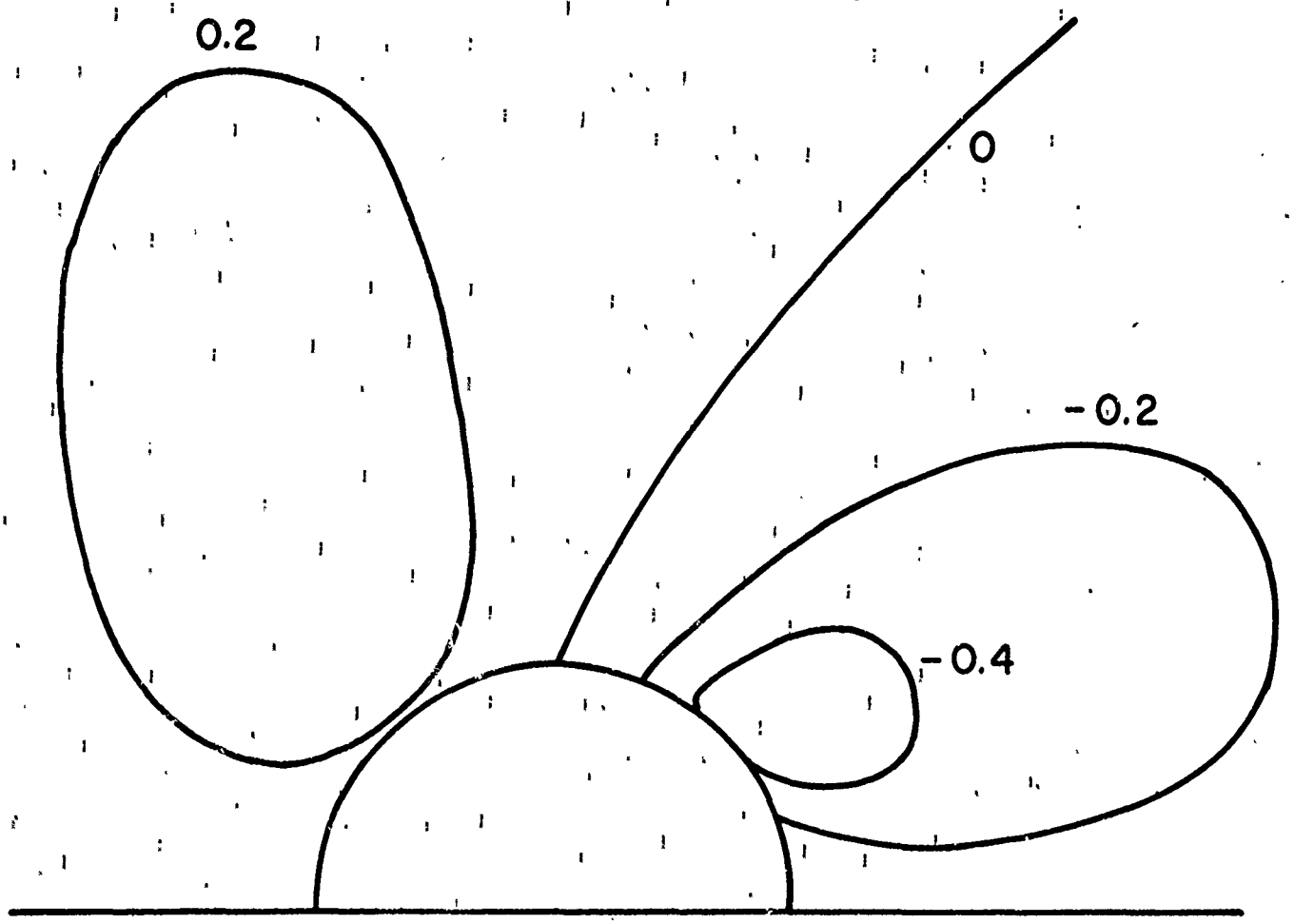

FIG. 8

FLOW PAST A CIRCULAR CYLINDER

$\lambda = 1 \quad Q_{\infty} = 1.5 \quad T_B = 1$

TEMPERATURE CONTOURS

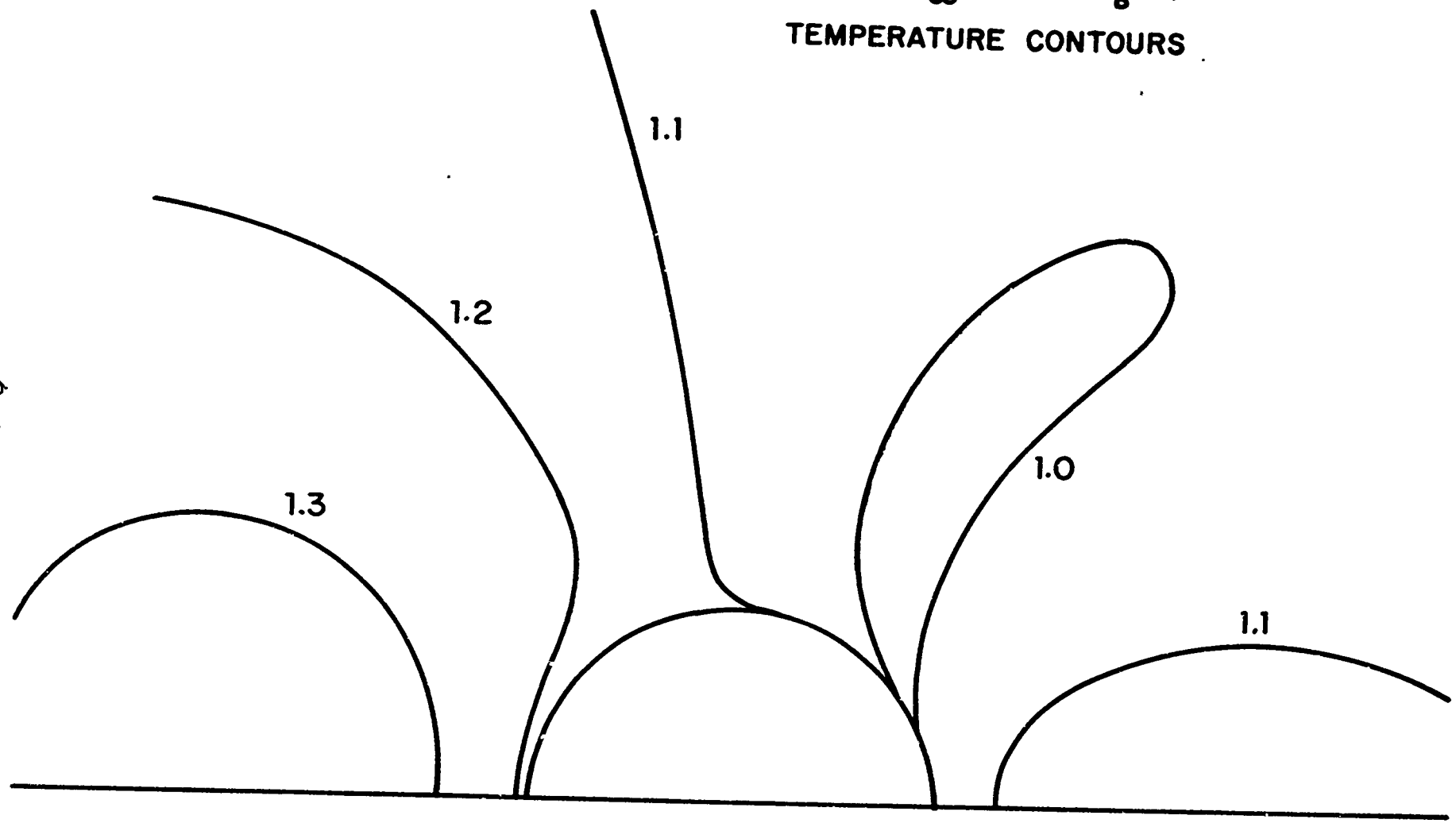

FIG. 9

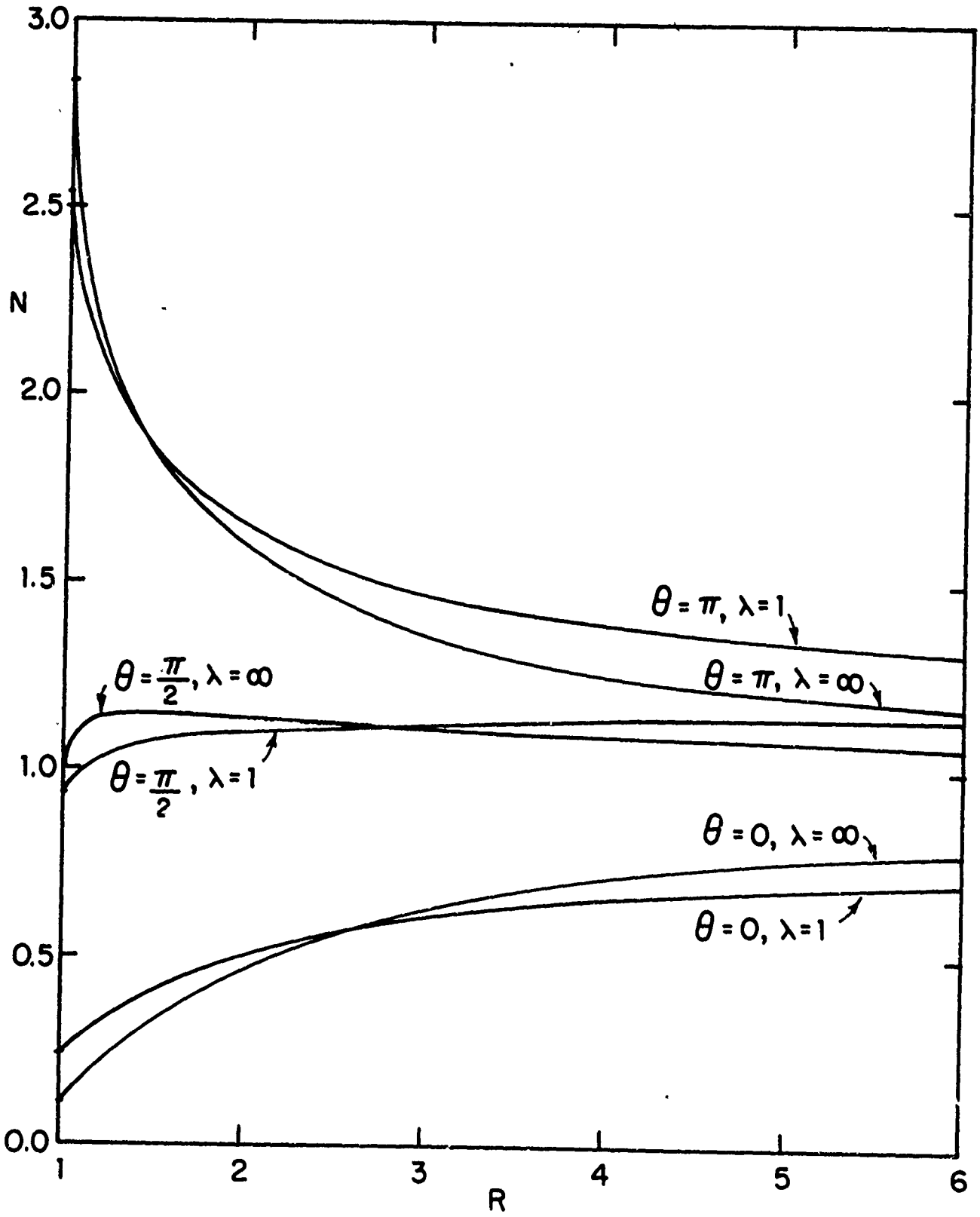

FIG. 10 DENSITY PROFILES
$Q_\infty = 1.5$, $T_B = 1$

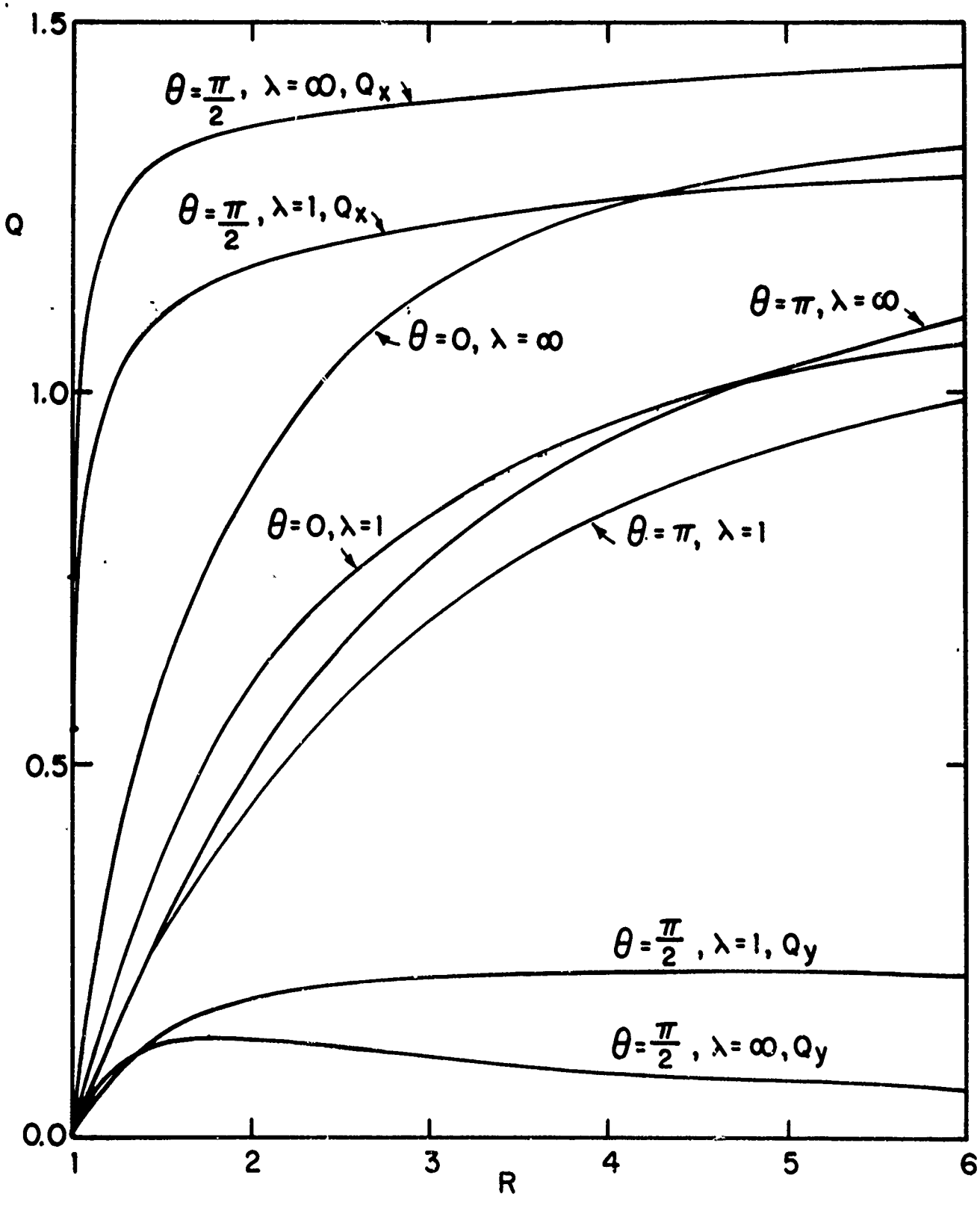

FIG. 11 VELOCITY PROFILES
$Q_\infty = 1.5$, $T_B = 1$

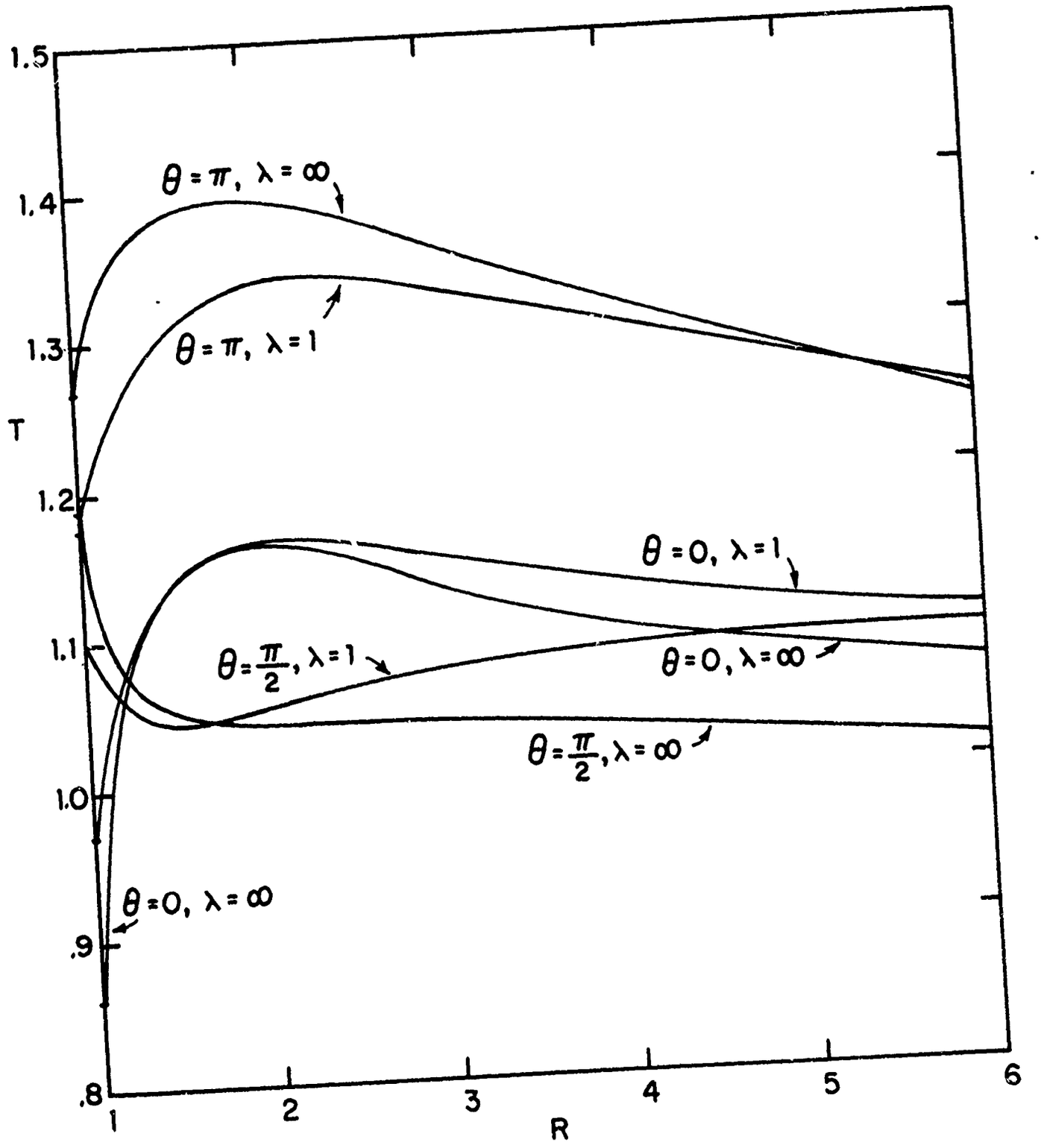

FIG. 12 TEMPERATURE PROFILES
$Q_\infty = 1.5$, $T_B = 1$

FLOW PAST AN ELLIPTIC CYLINDER

$\lambda = 1 \quad Q_\infty = 1 \quad T_B = 1$

DENSITY CONTOURS

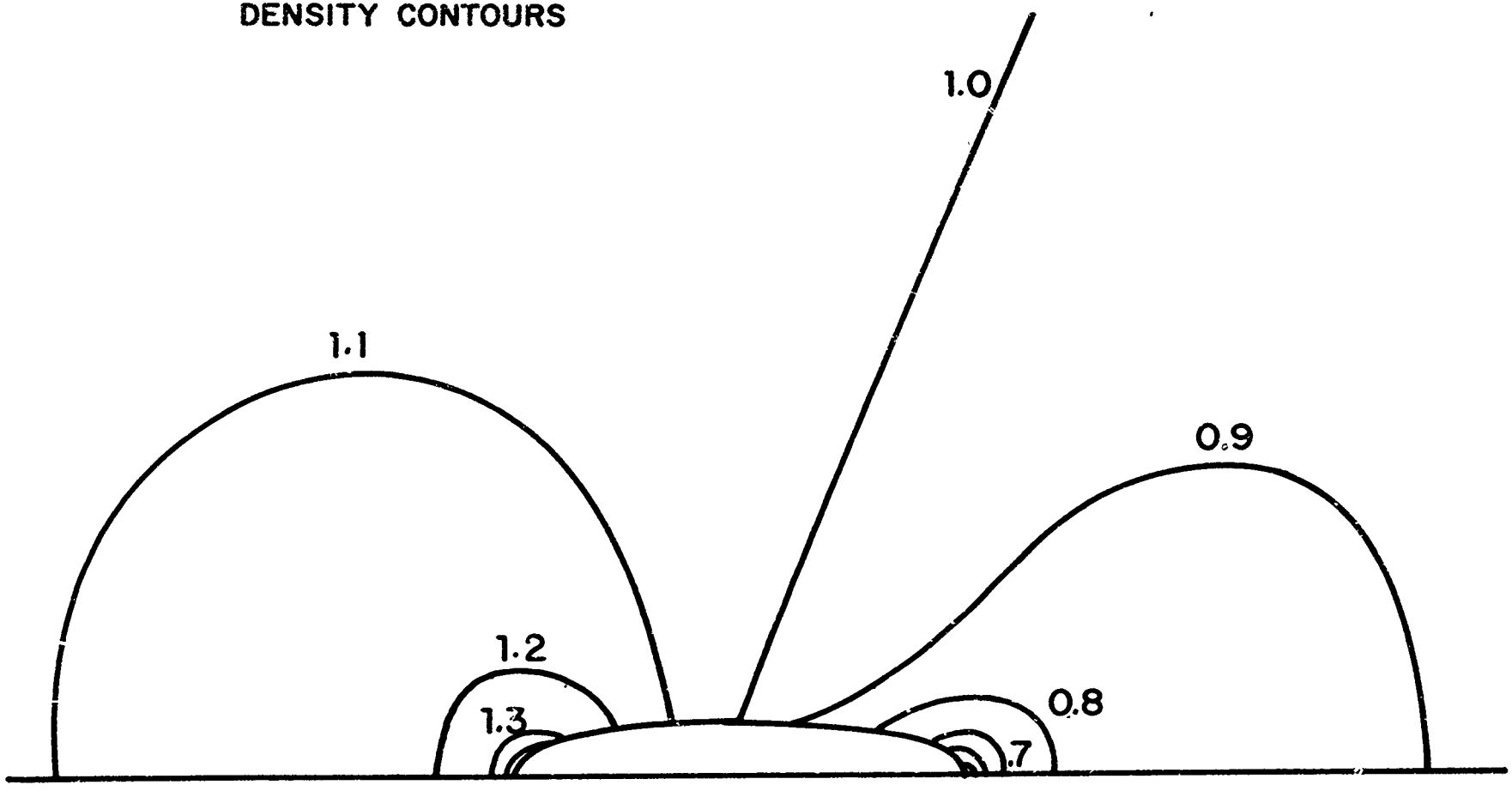

FIG. 13

FLOW PAST AN ELLIPTIC CYLINDER

$\lambda = 1 \quad Q_\infty = 1 \quad T_B = 1$

VELOCITY CONTOURS - Q_x

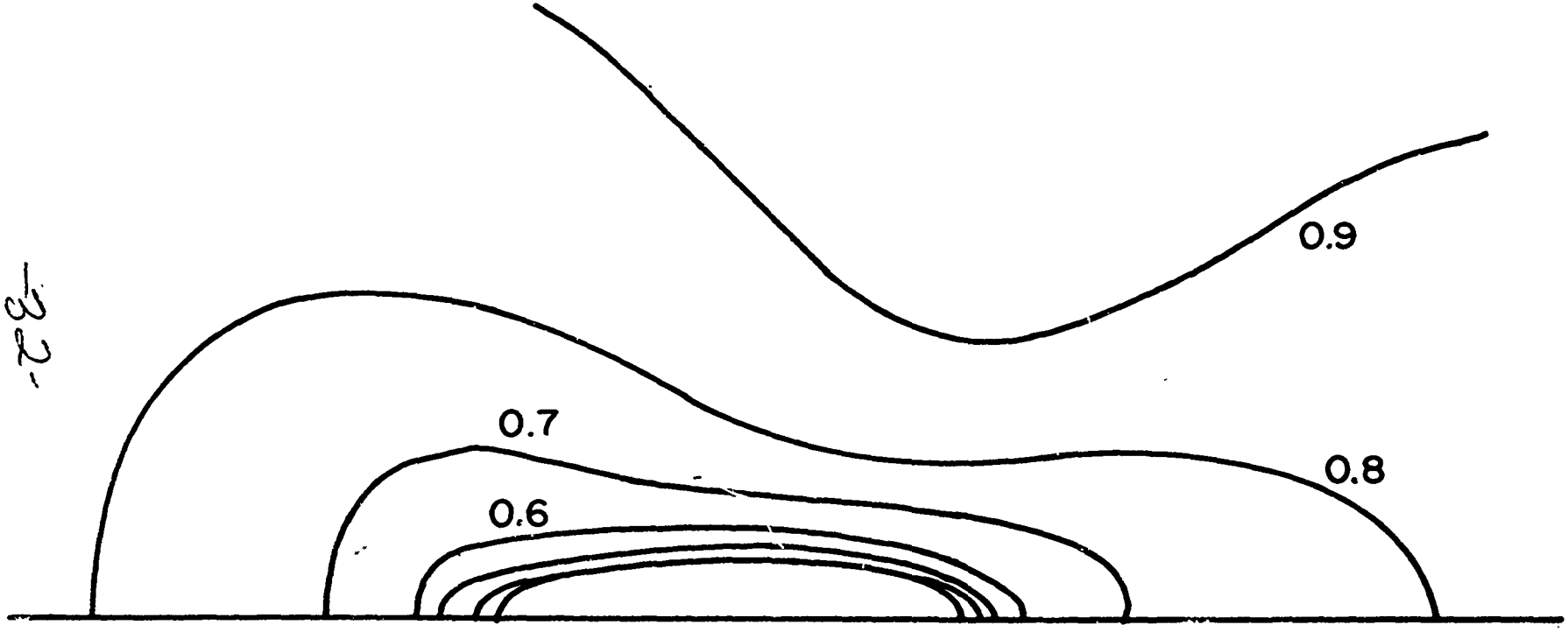

-32-

FIG. 14

FLOW PAST AN ELLIPTIC CYLINDER

$\lambda = 1 \quad Q_\infty = 1 \quad T_B = 1$

VELOCITY CONTOURS - Q_y

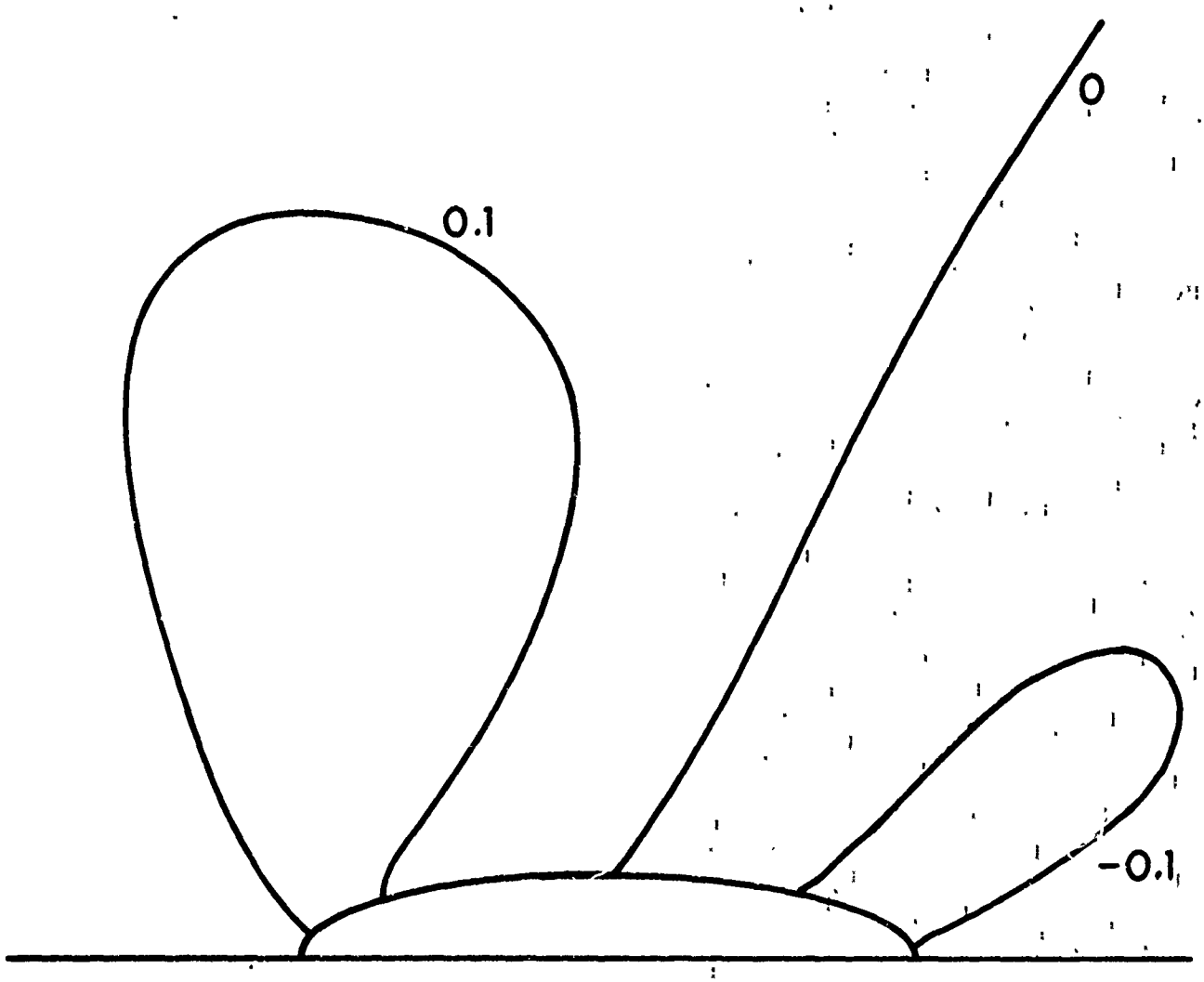

FIG. 15

FLOW PAST AN ELLIPTIC CYLINDER

$\lambda = 1 \quad Q_\infty = 1 \quad T_B = 1$

TEMPERATURE- CONTOURS

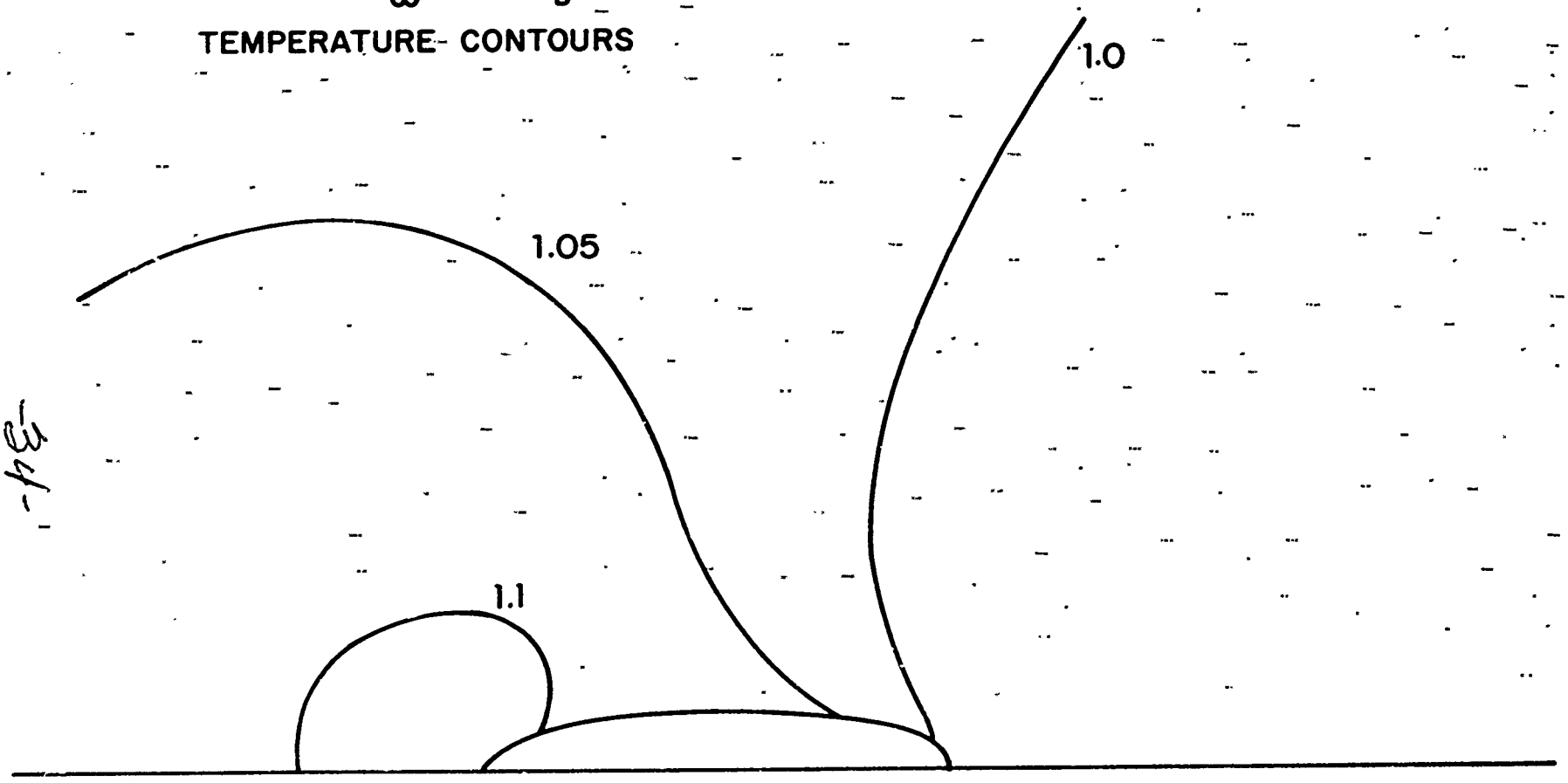

FIG. 16

FLOW PAST A FINITE FLAT PLATE

$\lambda = \infty \quad Q_\infty = 3 \quad T_B = 1$

DENSITY CONTOURS

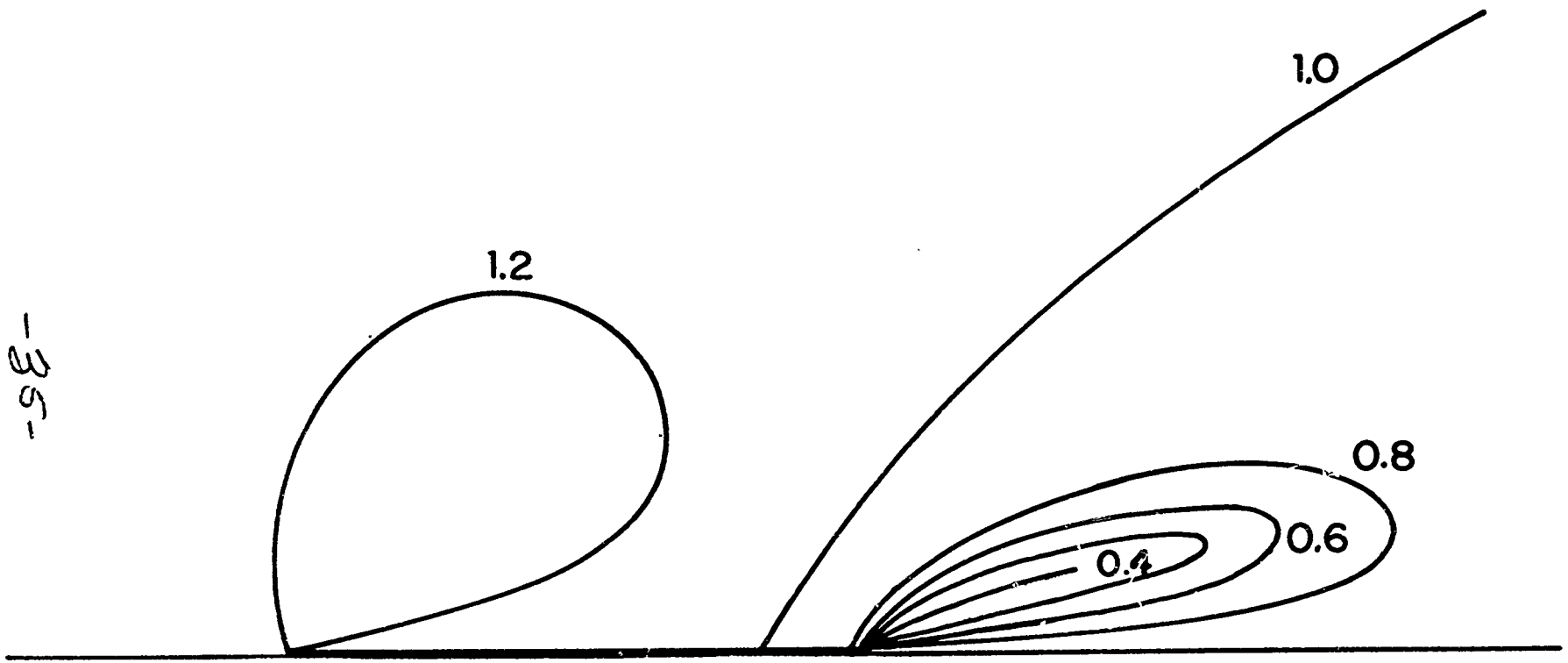

FIG. 17

FLOW PAST A FINITE FLAT PLATE

$\lambda = \infty \quad Q_\infty = 3 \quad T_B = 1$

VELOCITY CONTOURS - Q_x

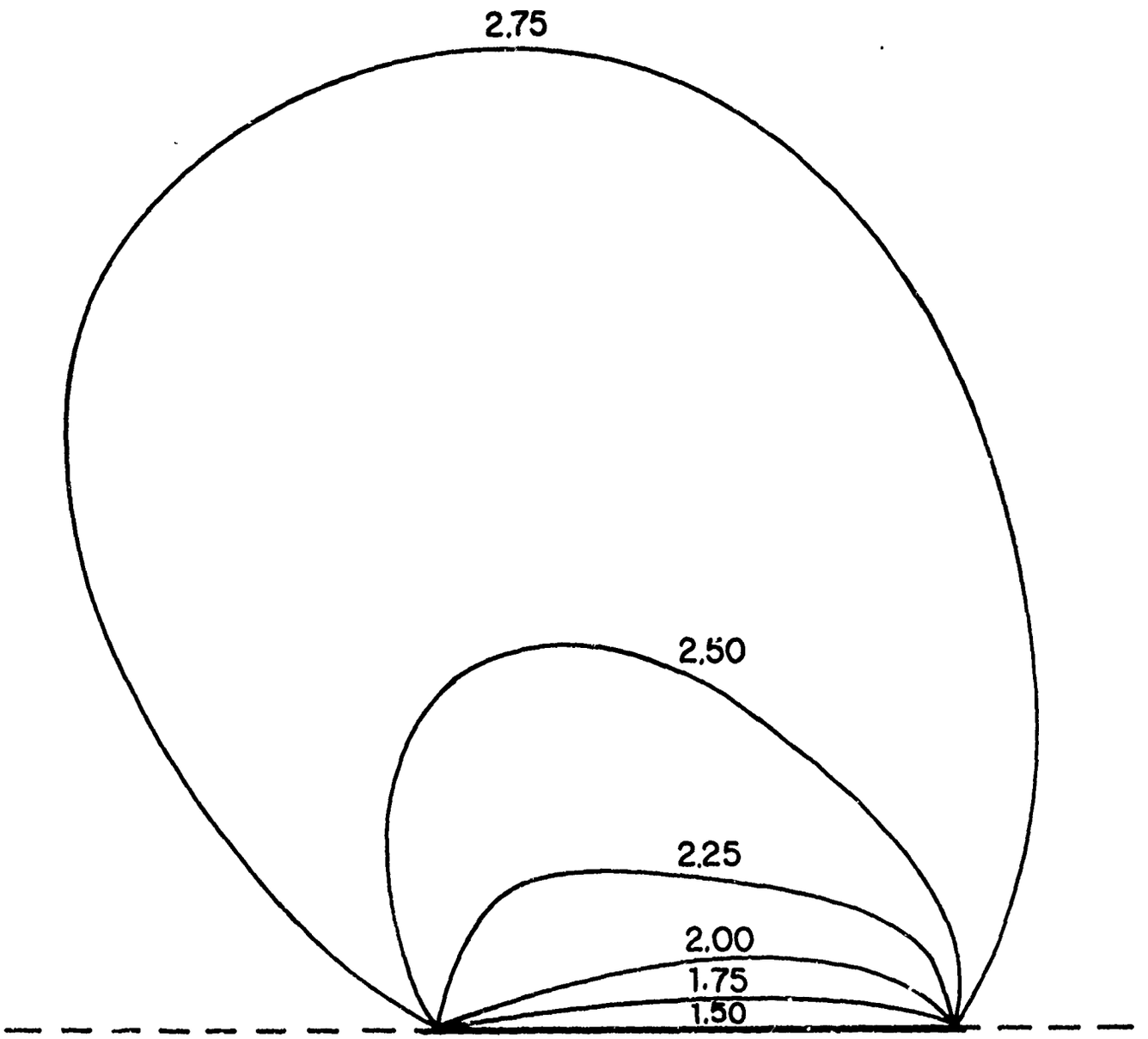

FIG. 18

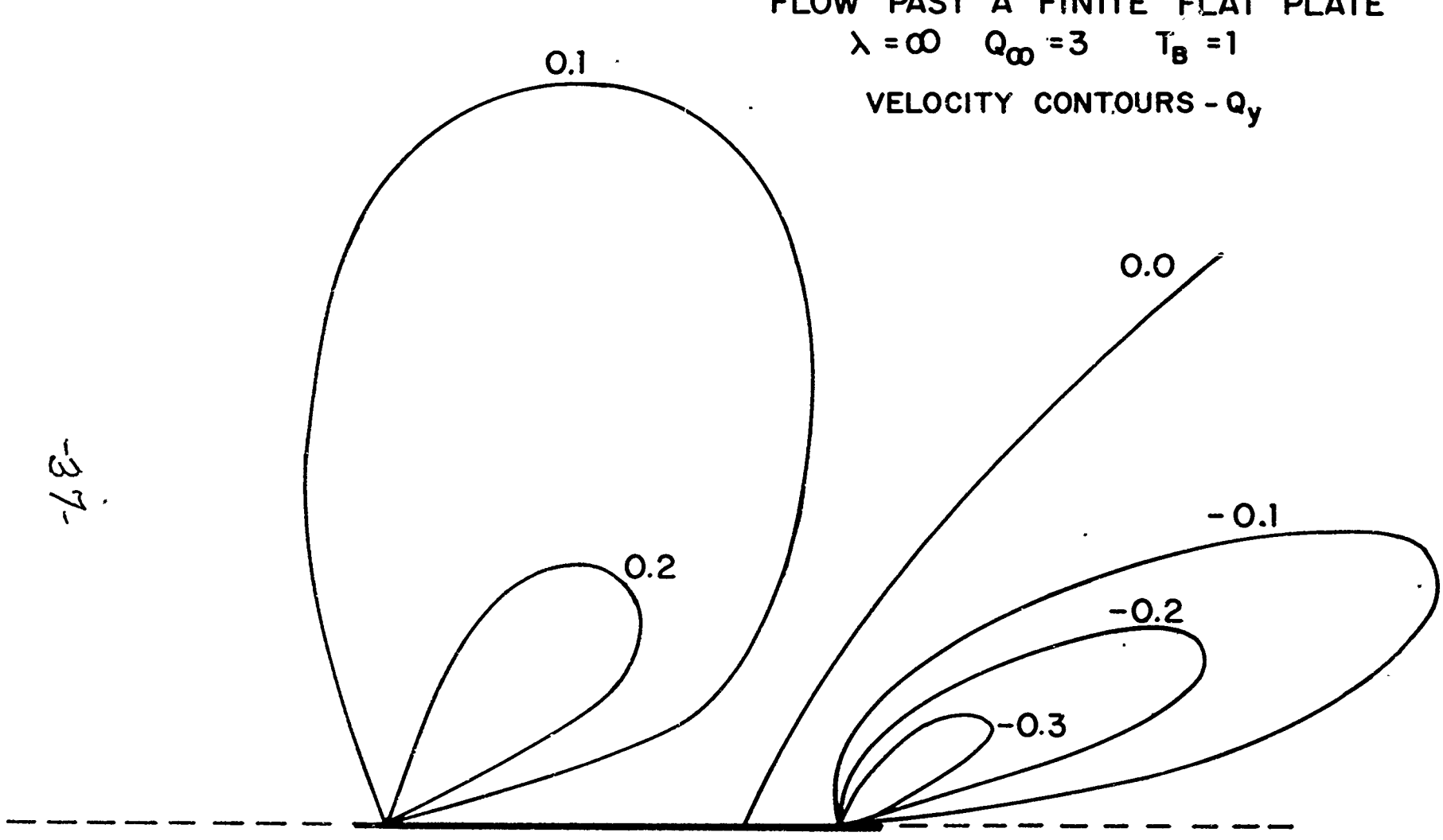
FLOW PAST A FINITE FLAT PLATE
λ = ∞ Q∞ = 3 TB = 1
VELOCITY CONTOURS - Qy
0.1
0.0
-0.1
0.2
-0.2
-0.3

FIG. 19

FLOW PAST A FINITE FLAT PLATE

$\lambda = \infty \quad Q_\infty = 3 \quad T_B = 1$

TEMPERATURE CONTOURS

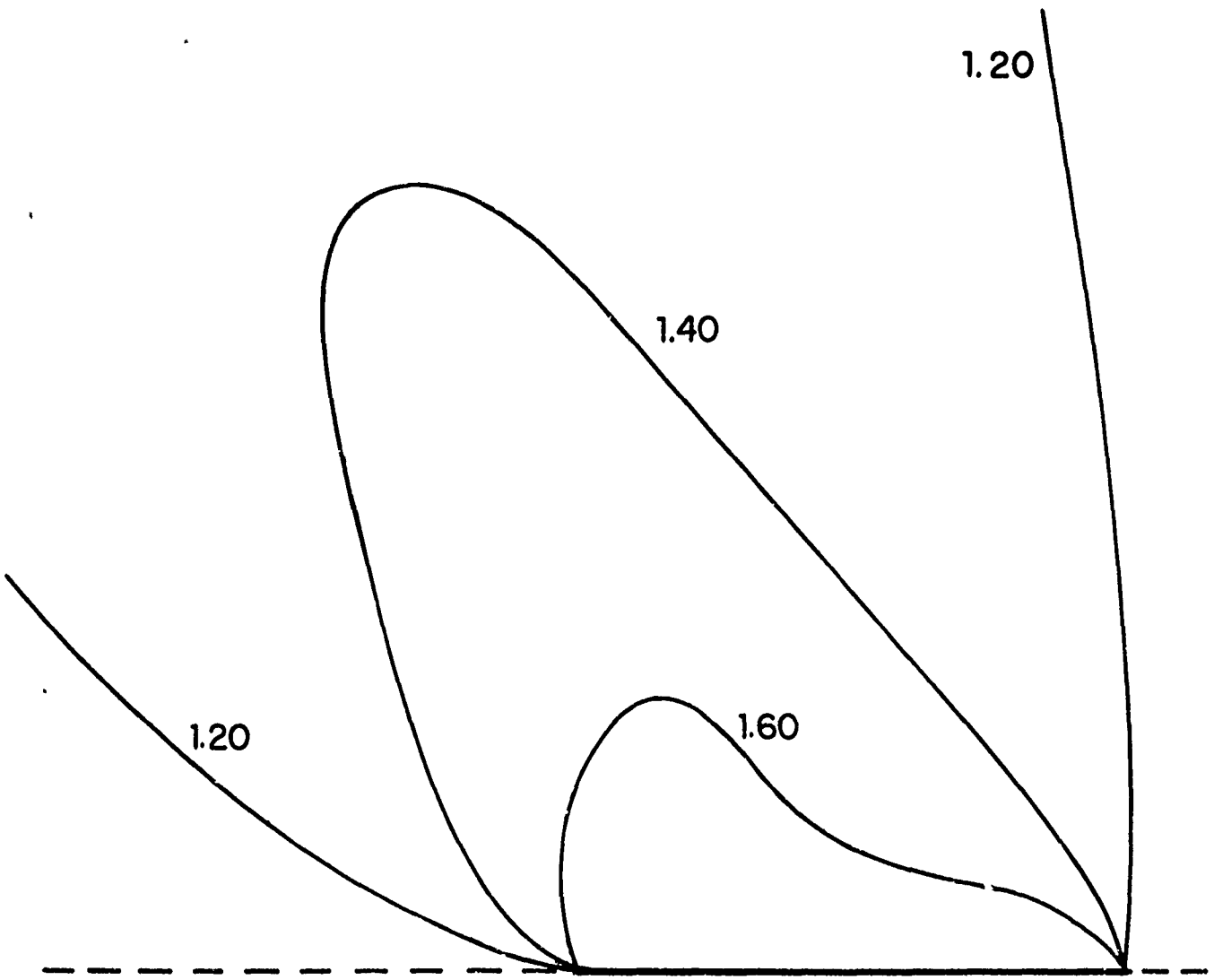

FIG. 20

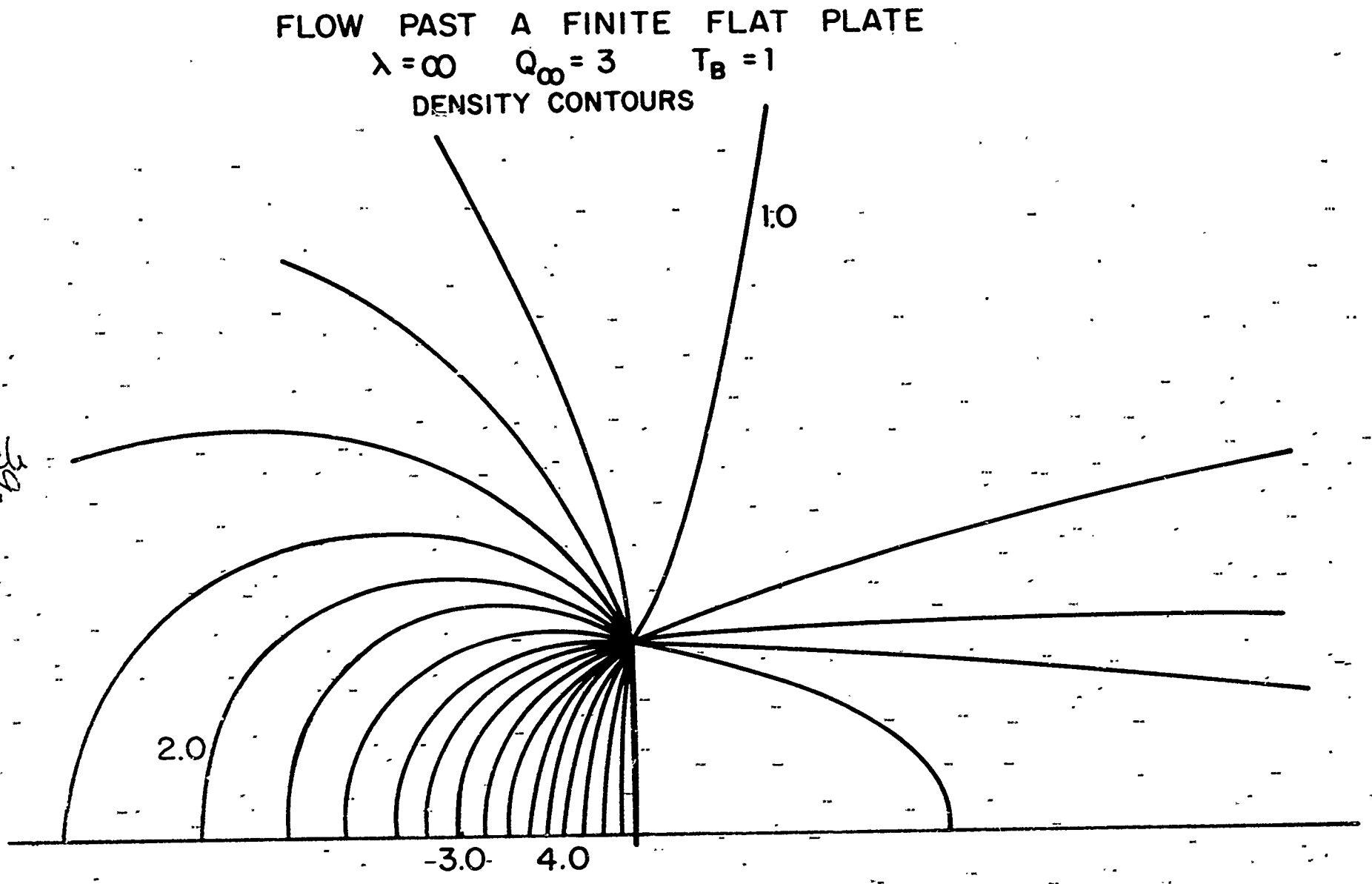
FLOW PAST A FINITE FLAT PLATE
$\lambda = \infty$ $Q_\infty = 3$ $T_B = 1$
DENSITY CONTOURS
1.0
2.0
-3.0-
4.0

FIG. 21

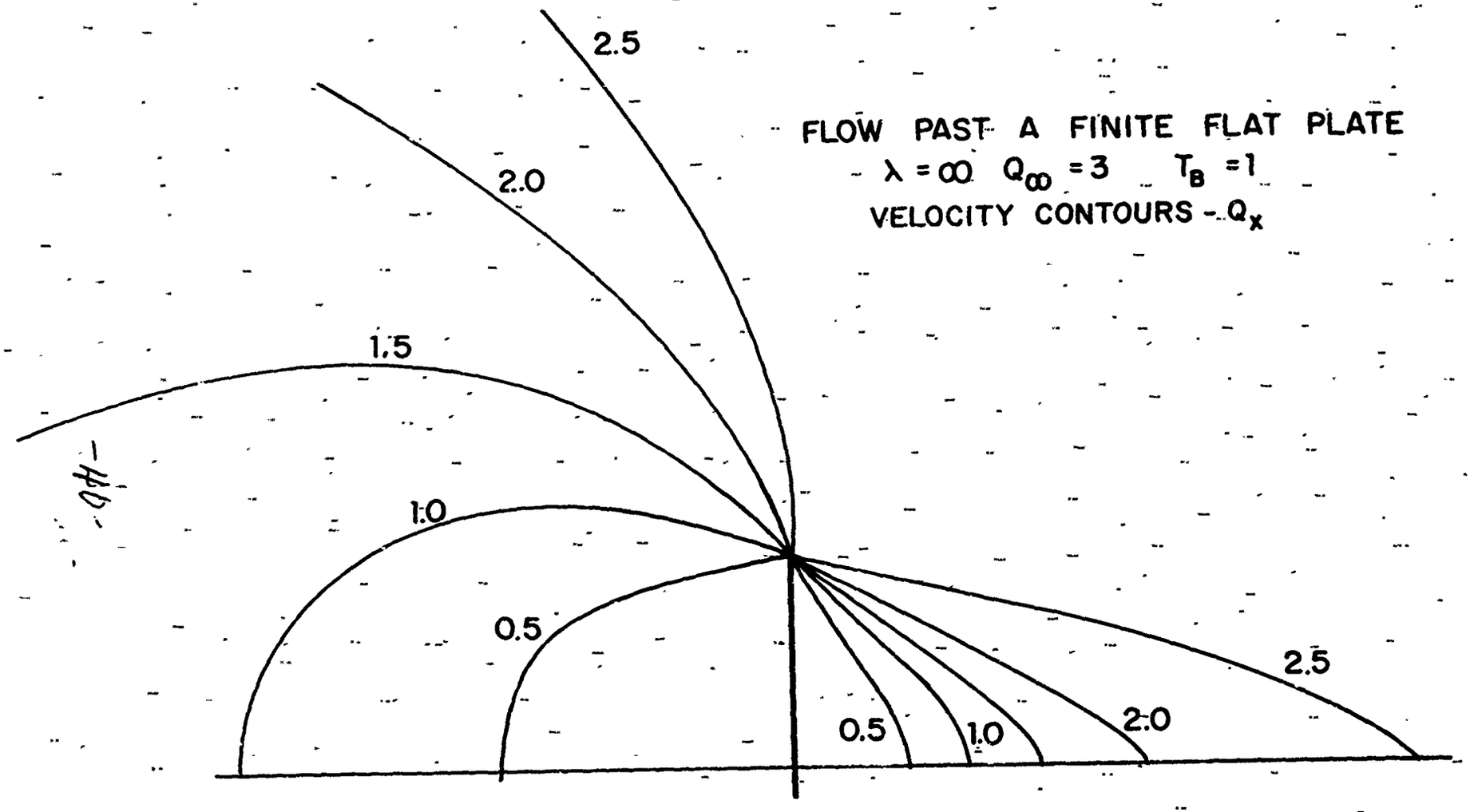
FLOW PAST A FINITE FLAT PLATE
λ = ∞ Q∞ = 3 TB = 1
VELOCITY CONTOURS - Qx
2.5
2.0
1.5
1.0
0.5
0.5
1.0
2.0
2.5

FIG. 22

FLOW PAST A FINITE FLAT PLATE

$\lambda = \infty \quad Q_\infty = 3 \quad T_B = 1$

VELOCITY CONTOURS - Q_y

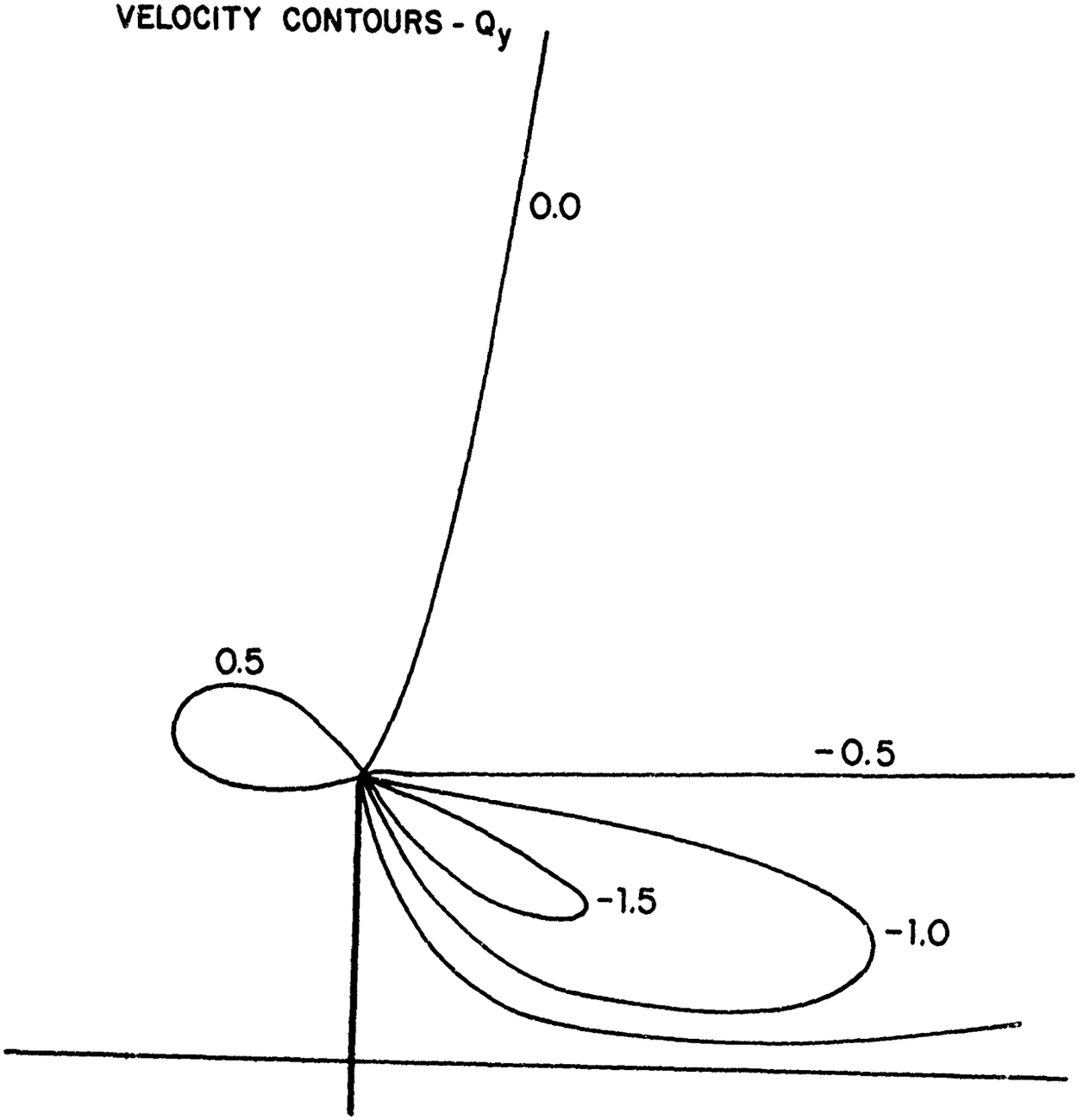

FIG. 23

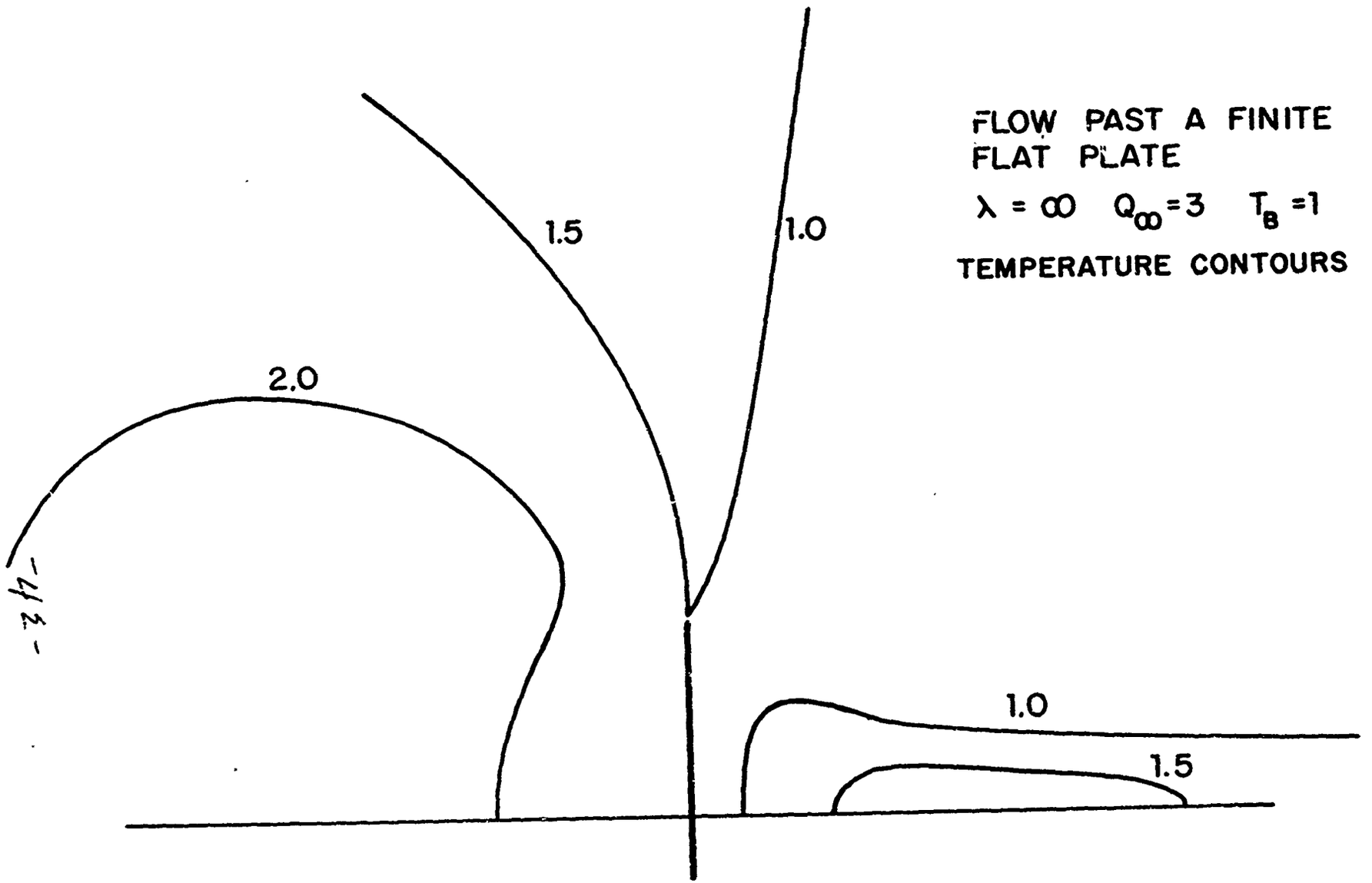
FLOW PAST A FINITE
FLAT PLATE
λ = ∞ Q∞ = 3 TB = 1
TEMPERATURE CONTOURS
1.5
1.0
2.0
1.0
1.5

FIG. 24